Geoscience Frontiers 7 (2016) 155–170

HOSTED BY

Contents lists available at ScienceDirect

China University of Geosciences (Beijing)

Geoscience Frontiers

journal homepage: www.elsevier.com/locate/gsf

Research paper

Exhuming the Meso–Cenozoic Kyrgyz Tianshan and Siberian Altai-Sayan: A review based on low-temperature thermochronology

Stijn Glorie [a,*], Johan De Grave [b]

[a] Centre for Tectonics, Resources and Exploration (TRaX), Department of Earth Sciences, School of Physical Sciences, The University of Adelaide, Adelaide SA 5005, Australia
[b] Dept. Geology & Soil Science, MINPET Group, Ghent University, 281-S8 Krijgslaan, Ghent 9000, Belgium

ARTICLE INFO

Article history:
Received 28 January 2015
Received in revised form
9 April 2015
Accepted 29 April 2015
Available online 13 May 2015

Keywords:
Central Asia
Tianshan
Altai Sayan
Thermochronology
Exhumation
Fault reactivation

ABSTRACT

Thermochronological datasets for the Kyrgyz Tianshan and Siberian Altai-Sayan within Central Asia reveal a punctuated exhumation history during the Meso–Cenozoic. In this paper, the datasets for both regions are collectively reviewed in order to speculate on the links between the Meso–Cenozoic exhumation of the continental Eurasian interior and the prevailing tectonic processes at the plate margins. Whereas most of the thermochronological data across both regions document late Jurassic–Cretaceous regional basement cooling, older landscape relics and dissecting fault zones throughout both regions preserve Triassic and Cenozoic events of rapid cooling, respectively. Triassic cooling is thought to reflect the Qiangtang–Eurasia collision and/or rifting/subsidence in the West Siberian basin. Alternatively, this cooling signal could be related with the terminal terrane-amalgamation of the Central Asian Orogenic Belt. For the Kygyz Tianshan, late Jurassic–Cretaceous regional exhumation and Cenozoic fault reactivations can be linked with specific tectonic events during the closure of the Palaeo-Tethys and Neo-Tethys Oceans, respectively. The effect of the progressive consumption of these oceans and the associated collisions of Cimmeria and India with Eurasia probably only had a minor effect on the exhumation of the Siberian Altai-Sayan. More likely, tectonic forces from the east (present-day co-ordinates) as a result of the building and collapse of the Mongol-Okhotsk orogen and rifting in the Baikal region shaped the current Siberian Altai-Sayan topography. Although many of these hypothesised links need to be tested further, they allow a first-order insight into the dynamic response and the stress propagation pathways from the Eurasian margin into the continental interior.

1. Introduction

The mountainous landscape of the Central Asian Tianshan and Altai-Sayan predominantly formed as a response to recurrent tectonic deformation (e.g. Hendrix et al., 1992; De Grave et al., 2007; Jolivet et al., 2013). The causes for these episodes of deformation are not yet fully understood. It has been suggested widely that the Meso-Cenozoic punctuated (viz., recurring at interrupted intervals) intracontinental deformation that affected Central Asia, is largely related with distant collisions at the southern Eurasian plate margin, with the most recent pulse of deformation being a far-field response to the India-Eurasia collision (e.g. Molnar and Tapponnier, 1975; Knapp, 1996; De Grave et al., 2007). The India-Eurasia collision not only caused shortening and uplift in the Himalayas and Tibet (e.g. Patriat and Achache, 1984; Harrison et al., 1992; Wang et al., 2001), but also the continuous convergence between India and Eurasia and the growth of the Tibetan Plateau induced convergence-drive (e.g. Abdrakhmatov et al., 1996) and/or flexure-related (Aitken, 2011) stresses that propagated into the Eurasian interior where they deformed the weaker crust of Central Asia (e.g. Knapp, 1996; Wang et al., 2001). Specifically, this deformation is preferentially accommodated by strength heterogeneities such as pre-existing fault zones within the crust of Tibet and Central Asia (e.g. England and Houseman, 1985), resulting in fault reactivation and associated rapid exhumation (Jolivet et al., 2001, 2010; Walker et al., 2007; Clark et al., 2010; Duvall et al., 2011; Glorie et al., 2011a, 2012a,b; Oskin, 2012; De Grave et al., 2013).

* Corresponding author. Tel.: +61 8 8313 2206.
E-mail address: stijn.glorie@adelaide.edu.au (S. Glorie).
Peer-review under responsibility of China University of Geosciences (Beijing).

http://dx.doi.org/10.1016/j.gsf.2015.04.003

The chronology and dynamics of the India-Eurasia convergence and collision as well as its influence on the exhumation of Tibet and Central Asia have been a matter of debate in recent years. Patriat and Achache (1984) were among the first to argue that the India-Eurasia collision occurred around ~50 Ma. Rowley (1996) and Clift et al. (2003) proposed a very similar age-estimate based on a review of stratigraphic data. However, more recent palaeomagnetic, biostratigraphic and sedimentological studies suggested that India and Eurasia were still distinctly separated at ~55–50 Ma and that the collision occurred around ~35 Ma (e.g. Aitchison et al., 2007). More specifically, Jiang et al. (2015) argued that a Tethyan seaway still existed between India and Eurasia until ~38–34 Ma, suggesting that the final collision of India with Eurasia must have occurred during or after the Priabonian. This late Eocene age for the collision was later confirmed by several others recent studies as well (e.g. Najman et al., 2010; Bouilhol et al., 2013). In addition, Van Hinsbergen et al. (2012) proposed a model involving two collisions: a 'soft' collision between Greater India and Eurasia at ~50 Ma and a 'hard' collision of India with Eurasia at ~25 Ma, suggesting that the collision is more complex than it was originally described.

Within southern Central Asia, widespread tectonic activity has been documented as transpiring since ~25 Ma (e.g. Hendrix et al., 1992; Yin et al., 1998) which corresponds well with the proposed timing of the 'hard' collision between India and Eurasia (Van Hinsbergen et al., 2012) as well as with the timing of enhanced crustal thickening in Tibet (e.g. Yin and Harrison, 2000). However, recent thermochronological data on major fault zones indicate that Cenozoic tectonic activity may have affected southern Central Asia since the early Eocene (~55–45 Ma) (e.g. Glorie et al., 2011a), intensifying during the late Oligocene–early Miocene (~25–20 Ma) and again during the late Miocene–early Pliocene (~10–3 Ma) as a response to subsequent regional shortening (e.g. Sobel et al., 2006; Macaulay et al., 2014).

The onset of major intra-plate mountain building within Central Asia however already occurred during the early Mesozoic (e.g. Dumitru et al., 2001; De Grave et al., 2007, 2011; Gorie et al., 2010). In fact, most of the Central Asian topography formed during the Mesozoic (De Grave et al., 2013; Jolivet et al., 2013). However, the dynamics of the pre-Himalayan tectonic uplift and deformation in Central Asia are not fully understood either. After a long period of Palaeozoic accretions (e.g. Xiao et al., 2004, 2010, 2013), the crustal architecture of Central Asia was episodically reactivated from the late Triassic onwards (e.g. Jolivet et al., 2007; De Grave et al., 2013). An important phase of regional late Jurassic–early Cretaceous uplift and exhumation has been documented throughout most of Central Asia, which is thought to be associated with the collisions of Gondwana-derived Cimmerian Blocks to Eurasia (e.g. Yin and Harrison, 2000; Jolivet et al., 2001) and/or the elusive Mongol-Okhotsk orogeny in the East (e.g. Cogné et al., 2005; Jolivet et al., 2009; Glorie et al., 2012a). Hence, in a similar way as described for the Cenozoic exhumation of Central Asia, stress-propagation from the southern Eurasian margin induced deformation and mountain building in Central Asia during the Mesozoic as well (e.g. De Grave et al., 2007; Glorie et al., 2010). The Mesozoic Central Asian mountainous landscape was likely widespread and may have been almost continuous from the southern plate margin at that time, to deep in the continental interior. In this regard, it has been suggested recently that much of the Tibetan topography already existed prior to the India-Eurasia collision (e.g. Clark, 2011; Hetzel et al., 2011). Furthermore, preserved early Mesozoic geomorphic features, such as internally drained plateaus or old erosion surfaces, testify to abundant Mesozoic topography in Central Asia as well (e.g. Hetzel et al., 2002; Jolivet et al., 2007; De Grave et al., 2011).

This paper aims to synthesise and discuss the exhumation history of two key-regions within the Central Asian edifice: (1) the Kyrgyz Tianshan (southern Central Asia; Figs. 1 and 2) the Siberian Altai (northern Central Asia; Fig. 1). Both regions will be examined and compared using a broad-scale multi-method thermochronology survey and focussing on (1) the regional relief, (2) major dissecting fault zones which record more recent exhumation events (e.g. Jolivet et al., 2010; Glorie et al., 2011a, 2012a,b) and (3) preserved landscape relics which archive more ancient exhumation events (e.g. Jolivet et al., 2007; De Grave et al., 2011). This approach enables a complete reconstruction of the thermal history and allows discussing the timing of punctuated reactivation events as a response to collisions and crustal shortening at the plate margins. It is furthermore attempted to comment on the timing and extent of Mesozoic and Cenozoic deformation within Central Asia as a response to distant tectonic activity at the Eurasian margins.

2. Thermochronological datasets

During the last decade, the Kyrgyz Tianshan and Siberian Altai-Sayan have been studied intensively, resulting in several recent publications of extensive thermochronological datasets. This

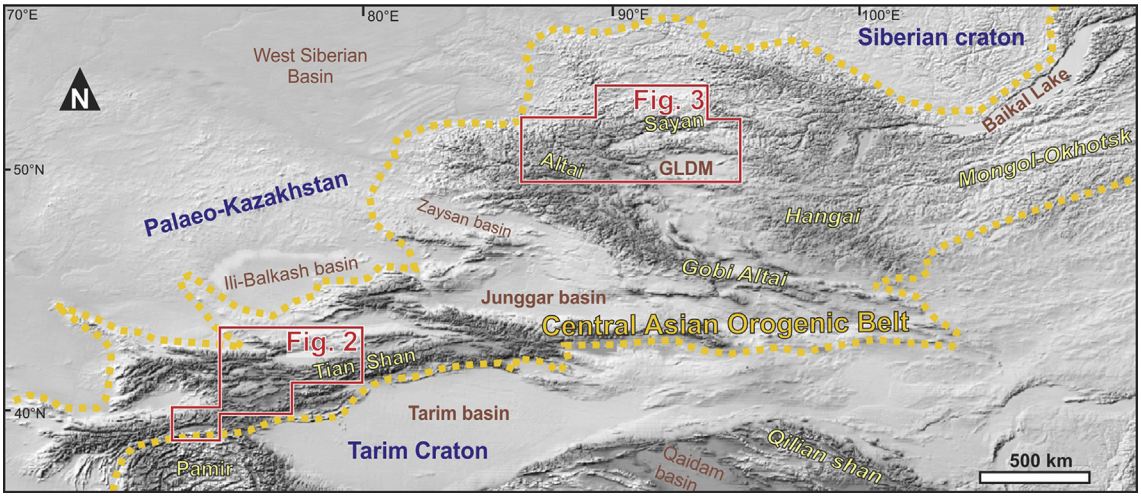

Figure 1. Digital elevation map of the Central Asian Orogenic Belt (CAOB) with indication of the study areas for this paper: the Siberian Altai-Sayan and the Kyrgyz Tianshan. Both locations occupy key-positions in the northern and southern CAOB respectively and both hold major suture-shear zones that were reactivated during the Meso–Cenozoic.

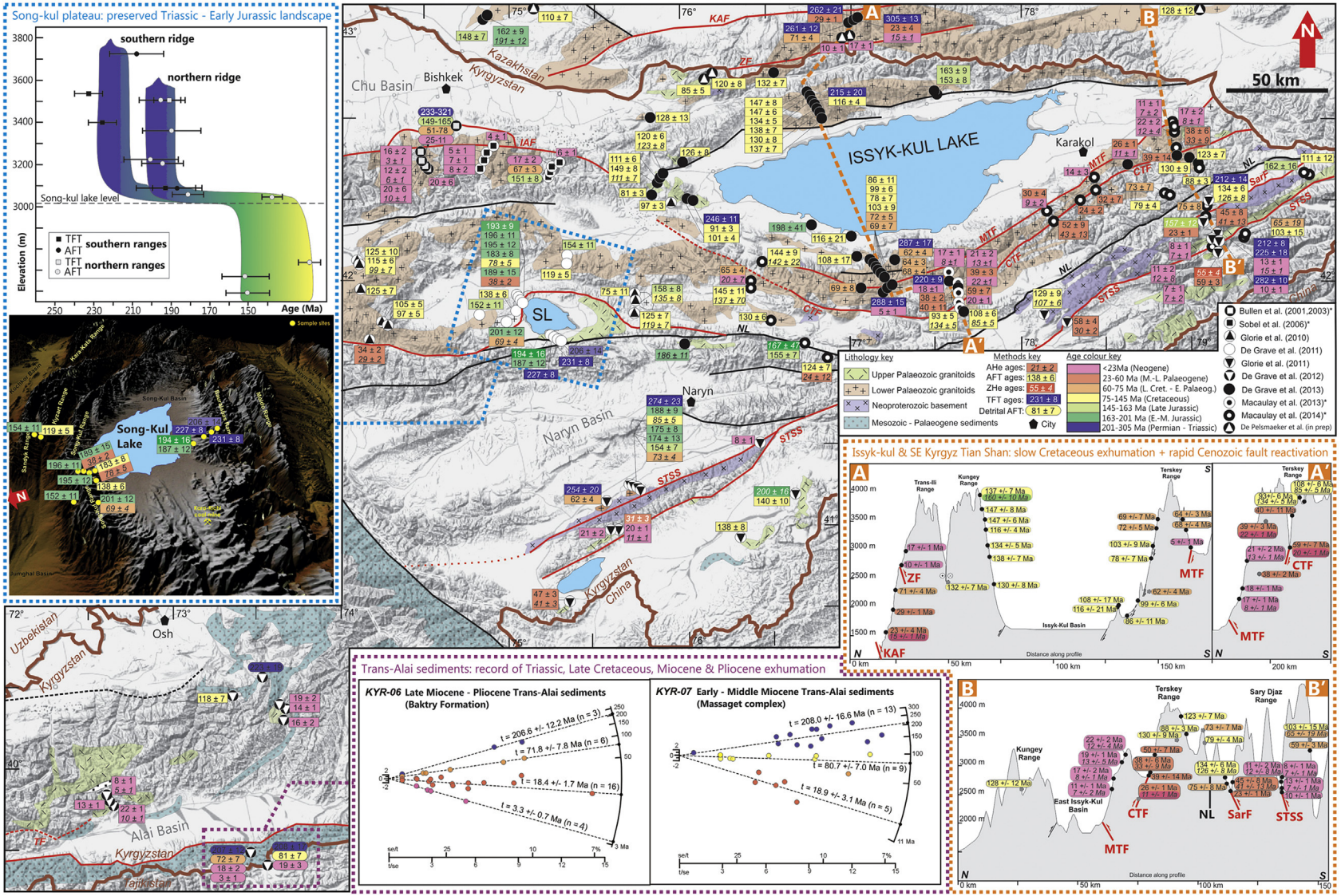

Figure 2. Digital elevation model for the Kyrgyz Tianshan with indication of geological feature (major structures, granitoid intrusions, Precambrian basement rocks and Mesozoic–Palaeogene sediments) and thermochronological ages from Bullen et al. (2001, 2003); Sobel et al. (2006); Glorie et al. (2010, 2011a); De Grave et al. (2011, 2012, 2013); Macaulay et al. (2013, 2014); De Pelsmaeker et al. (2015). Thermochronological ages (TFT in white font, ZHe in white underlined/italic, AFT in black font, AHe underlined/italic) are colour coded into major age-groups (purple = Permian–Triassic, green = Jurassic, yellow = Cretaceous, orange = late Cretaceous–early Palaeogene, red = Palaeogene, pink = Neogene). Where multiple consistent data was obtained for the same location, an average is given. Structures for which late Cretaceous–Cenozoic (partially) reset ages were obtained are displayed in red (STSS = South Tianshan Suture, SarF = Sarydjaz Fault, NL = Nikolaev Line, CTF = Central Terskey Fault, MTF = Main Terskey Fault, ZF = Zaili Fault, KAF = Karakunug-Almaty Fault–simplified after De Grave et al., 2013; Macaulay et al., 2014). **Blue outlined insets**: 3D elevation model and age-elevation profiles for the Song-kul plateau. The age-elevation trends are coloured following the colour-code of the major age-groups and show preserved fast cooling/exhumation during the Triassic and reactivation during the late Jurassic – early Cretaceous (modified from De Grave et al., 2011). **Orange outlined insets**: Simplified cross-section through the topography surrounding lake Issyk-kul (orange dashed lines on the map) with indication of thermochronological data (vertical sample sections). Samples taken from the fault-escarpments show clear evidence for Cenozoic fault-induced exhumation during the Oligocene (CTF, SarF, KAF) and late Miocene–Pliocene (ZF, MTF and STSS). The Nikolaev line (NL) shows no evidence for Cenozoic fault-reactivation (modified from De Grave et al., 2013). **Purple outlined insets**: Radial plots (Vermeesch, 2009) for AFT ages obtained for Cenozoic sediments from the Trans-Alai region. Data is coloured following the colour-code of the major age-groups. These plots record exhumation of the southwest Tianshan during the Triassic, late Cretaceous, Miocene and Pliocene.

section aims to synthesise the data from Bullen et al. (2001, 2003), Sobel et al. (2006), Glorie et al. (2010, 2011a), De Grave et al. (2011, 2012, 2013), Macaulay et al. (2013, 2014) and De Pelsmaeker et al. (2015) for the Kyrgyz Tianshan and from De Grave and Van den haute (2002), De Grave et al., 2007, 2008, 2009, 2014) and Glorie et al. (2012a) for the Siberian Altai-Sayan in order to examine and compare the cooling and exhumation history of both regions on a regional scale. Figs. 2 and 3 show simplified geological maps of the basement architecture of the Kyrgyz Tianshan and Siberian Altai-Sayan respectively, superimposed on digital elevation models (refer to Fig. 1 for their location within Central Asia). Multi-method cooling ages (thermochronometric age data) are indicated and colour coded to identify regional trends in the dataset. Apatite fission track (AFT) ages are most common on the map and register the timing of thermal events through ~60–120 °C (e.g. Wagner and Van den haute, 1992 and references therein). Additional titanite fission track (TFT) ages date the timing of thermal events between ~275–285 °C (e.g. Kohn et al., 1993; Jacobs and Thomas, 2001). Where available, apatite (AHe) and zircon (ZHe) U-Th-Sm/He cooling ages are shown, indicating the timing of thermal events between ~45–75 °C for apatite (e.g. Ehlers and Farley, 2003) and ~170–190 °C for zircon (e.g. Reiners et al., 2004). More recent studies however indicate that the closure temperature of the ZHe system is dependent on the level of radiation damage (which is largely a function of the Uranium concentration) and can vary at least between ~130–200 °C (e.g. Wolfe and Stockli, 2010). The sections below discuss the regional trends in the thermochronological data and aim to connect the resulting thermal history of the Kyrgyz Tianshan and the Siberian Altai-Sayan with tectonic events at the plate margins. The reader is referred to the references listed above for more details on the individual datasets.

2.1. Low-temperature thermochronology of the Kyrgyz Tianshan

Throughout the entire Kyrgyz Tianshan, a large number of late Jurassic–Cretaceous (~160–80 Ma) AFT (and more limited ZHe and AHe) ages were obtained (Fig. 2: pale green and yellow ages). These cooling ages dominate in the middle Kyrgyz Tianshan, especially along the northern and western margin of lake Issyk-kul and between the South Tianshan Suture (STSS) and the Central Terskey Fault (CTF; Fig. 2). In the southwest, the basement is largely covered by thick deposits of Meso–Cenozoic sediments and thermochronological data on exposed basement rocks is thus largely lacking. However, for few isolated granitoid outcrops in the southwest, similar late Jurassic–Cretaceous cooling ages were obtained, indicating that most of the Kyrgyz Tianshan basement exhumed during the Mesozoic (e.g. De Grave et al., 2013). For some areas within the Kyrgyz Tianshan edifice, anomalously older cooling ages were found. Titanite (TFT) and apatite (AFT) fission track data from the Song-kul plateau (insets left in Fig. 2) yield middle to late Triassic (~231–193 Ma) and late Triassic–early Jurassic basement ages (~206–183 Ma) respectively (Fig. 2: green and purple ages). Similar early Jurassic (~188–174 Ma) AFT ages were obtained just north of the South Tianshan Suture at the margin of the Naryn Basin (Fig. 2). These ages suggest local preservation of early Mesozoic Kyrgyz Tianshan relief (De Grave et al., 2011; Glorie et al., 2011a). Although these older relief expressions are only locally preserved, the region of preserved Triassic–early Jurassic could be more extensive, spanning most of the covered basement underneath the Naryn Basin (Fig. 2).

Along several E–W striking fault zones, much younger, Cenozoic AFT, ZHe and AHe ages were obtained (Fig. 2: red and pink ages). These faults are colour coded in red in Fig. 2. For the South Tianshan Suture (STSS), cooling ages range from ~60 to ~7 Ma with the older (early Palaeogene: ~60–50 Ma) ages at higher elevations and the younger (late Palaeogene–Neogene: ~30–7 Ma) ages at lower elevations within the fault escarpments (Fig. 2: map and profile B–B′; Glorie et al., 2011a). Within the exposed sections along the Sarydjaz Fault (SarF), Eocene–Oligocene cooling ages were obtained (~45–23 Ma) with the youngest (~23 Ma) at lower elevations (Glorie et al., 2011a; Macaulay et al., 2014). The Central (CTF) and Main (MTF) Terskey Fault yield Cenozoic cooling ages as well. Within the CTF, Palaeogene AFT ages were obtained ranging from ~60 Ma at high elevations until ~26 Ma at lower elevations. AHe ages for the same samples are generally younger and range from ~20–11 Ma. For the MTF, mainly Neogene AFT and AHe ages were obtained ranging from ~22 to ~7 Ma in vertical profile (Fig. 2: map and profile B–B′). Note that the sense of displacement changes along strike of the CTF (e.g. De Grave et al., 2013; Macaulay et al., 2013). In the west, the cooling ages along the CTF escarpment change abruptly from ~65 to ~5 Ma (Fig. 2: map and profile A–A′). Within the southern slopes of the Kyrgyz Range (south of the Issyk-Ata (IAF) Fault, NW in Fig. 2) and the Alai Range (north of the Turkestan Fault (TF), SW in Fig. 2), cooling ages range from ~25–4 Ma (Bullen et al., 2001, 2003; Sobel et al., 2006). In the vicinity of the Zaili (ZF) and Karakung-Almaty (KAF) faults in the far north of the map (Fig. 2: near the Kyrgyz-Kazakh border), cooling ages of ~17–10 and ~29–15 Ma were found respectively (De Grave et al., 2013; De Pelsmaeker et al., 2015). Hence most of the exposed flanks of faulted blocks throughout the Tianshan yield a Palaeogene and/or Neogene cooling signal. At the summits of the faulted blocks throughout the entire study area, cooling ages mainly vary from ~120 Ma (i.e. a preserved Cretaceous signal) to ~60 Ma.

Thermochronological data on detrital sediments within the intramontane basins in the Kyrgyz Tianshan are far less abundant and limited to a few ages from Neogene sediments in the Alai and Ferghana Basin (Fig. 2: near the Kyrgyz-Tajik border; De Grave et al., 2012) and the Chu Basin (Fig. 2: north of the IAF; Bullen et al., 2001). The main age components are similar in both basins, indicating cooling at ~230–200, ~165–145, ~80–65, ~50, ~25–10, and ~5–3 Ma, mimicking the cooling signals observed in the basement.

2.2. Low-temperature thermochronology of the Siberian Altai-Sayan

For the Siberian Altai-Sayan almost exclusively Cretaceous–ealry Palaeogene (~135–55 Ma) AFT and AHe cooling ages were obtained (Fig. 3: yellow and orange ages). Available TFT cooling ages within the Siberian Altai are significantly older and range between the early Permian (~299 Ma) and early Jurassic (~190 Ma) (Fig. 3: green and purple ages). Interestingly, a distinctive trend can be observed within the geographic distribution of both the AFT and TFT datasets. Where early–'middle' Cretaceous (~130–75 Ma) AFT and Permian–middle Triassic (~299–230 Ma) TFT cooling ages are found throughout the entire study area, the younger late Cretaceous–early Palaeogene (~75–55 Ma) AFT and late Triassic–early Jurassic (~225–190 Ma) TFT ages occur only in close vicinity to or within major fault zones (Glorie et al., 2012a; De Grave et al., 2014). This is illustrated in Fig. 3 by the occurrence of the orange-coded cooling ages near the Charysh-Terekta-Ulagan-Sayan Suture (CTUSS) (Glorie et al., 2012a), the West Sayan fault zone (De Grave et al., 2014), and the fault-bounded margins of the Teletskoye Basin (De Grave et al., 2009) and a fault branch of the Shapshal fault zone (De Grave et al., 2014) (Fig. 3). These fault systems are colour coded in red as they show evidence for late Cretaceous–Palaeogene fault activity. In addition, age-elevation profiles for the Siberian Altai indeed show more rapid cooling trends within the fault zones during the late Triassic–early Jurassic and during the late Cretaceous–early Palaeogene (Fig. 3: inset).

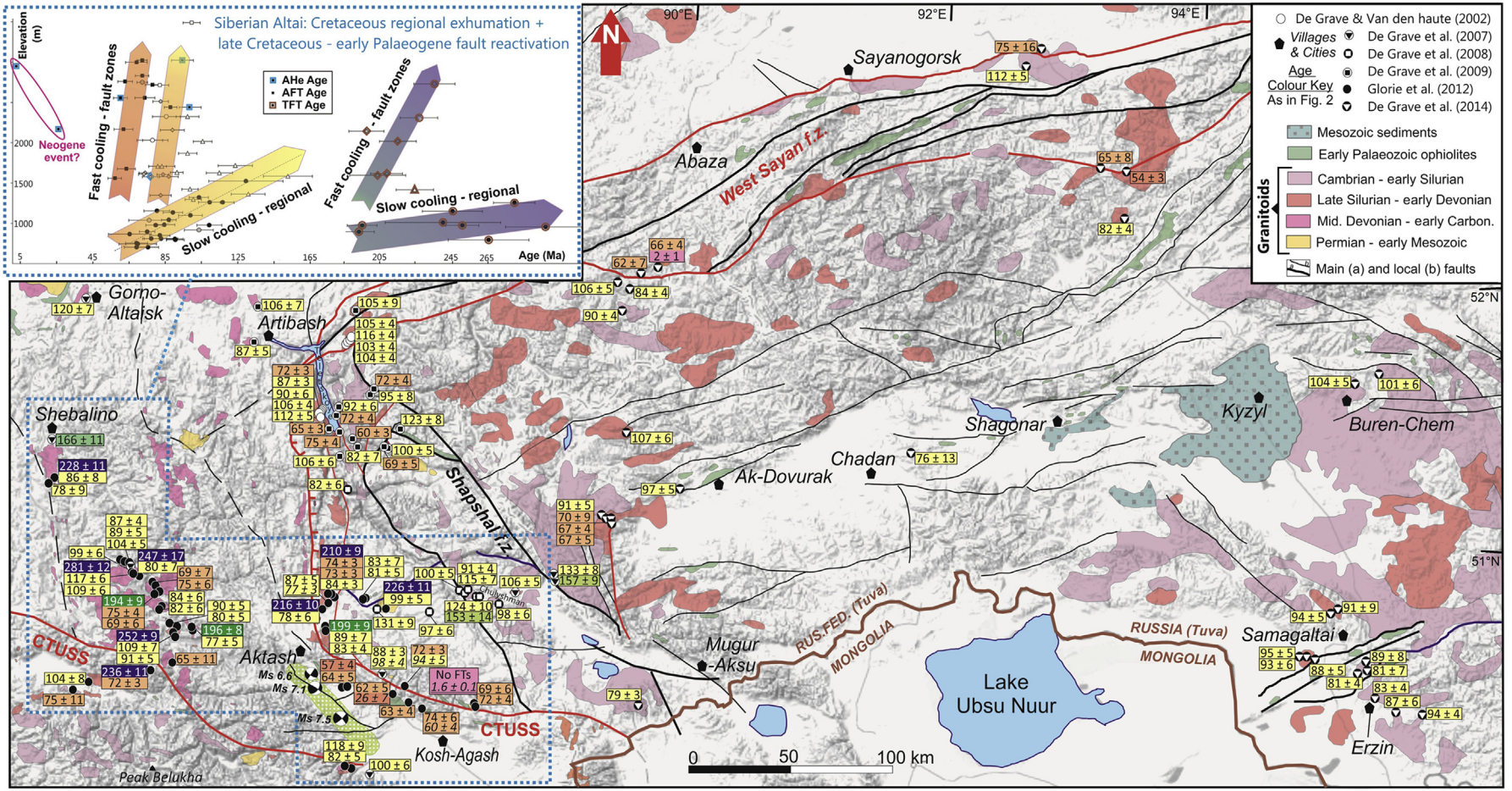

Figure 3. Digital elevation model of the Siberian Altai-Sayan with indication of geological features (major structures, granitoid intrusions, ophiolite rocks and Mesozoic sediments) and thermochronological ages from De Grave and Van den haute (2002); De Grave and Buslov (2007, 2008, 2009, 2014); Glorie et al. (2012a). The thermochronological ages (TFT in white font, AFT in black font, AHe in underlined/italic font) are colour coded into major age-groups (purple = Permian–Triassic, green = Jurassic, yellow = Cretaceous, orange = late Cretaceous–early Palaeogene, red = Palaeogene, pink = Neogene). Structures for which late Cretaceous–Cenozoic (partially) reset ages were obtained are displayed in red. **Inset**: Age-elevation profiles for the Siberian Altai (area contoured by blue dashed lines) showing nearly horizontal trends for the regional TFT and AFT data and nearly vertical trends for the TFT, AFT and AHe data obtained along major fault zones. The age-elevation trends are coloured following the colour-code of the major age-groups and indicate major fault activity during the early Jurassic and late Cretaceous–early Palaeogene (modified from Glorie et al., 2012a).

Few regions yield slightly older AFT cooling ages. For the Chulyshman plateau (bordered by the Shapshal fault zone in the east), late Jurassic–early Cretaceous (~155–100 Ma) cooling ages were obtained which are thought to reflect preservation of slightly older relief within the Siberian Altai (De Grave et al., 2008), similar as described for the Song-kul plateau in the Kyrgyz Tianshan.

At two locations along the CTUSS and the West Sayan fault zone, anomalously young (late Oligocene: ~26 Ma and Pleistocene: 2–1 Ma) AHe data were obtained (Glorie et al., 2012a; De Grave et al., 2014). The significance of these young ages is debatable given their low reproducibility, however they may indicate that Neogene fault activity may have reset the AHe clocks during the Pleistocene. These ages are however confirmed by Quaternary (~2.5–0.2 Ma) $^{40}Ar/^{39}Ar$ ages on paralavas (combustion metamorphism) within the Kuznetsk Coal Basin (branch of the West-Siberian basin, just north of the Altai-Sayan study area; Fig. 1) and the Junggar basin (just south of the Altai-Sayan study area; Fig. 1) (Novikov et al., 2008, in review). These observations together with the occurrence of recent fault activity along e.g. the CTUSS (Fig. 3: Chuya basin seismic zone; Lunina et al., 2008) and displaced Quaternary glacial features (Dehandschutter et al., 2002) suggest that the Altai-Sayan is affected by neotectonic (especially Pleistocene to recent) fault-reactivations.

3. Regional versus fault-induced cooling

As discussed above, for both the Kyrgyz Tianshan and Siberian Altai-Sayan, the youngest thermochronometric data were generally obtained within major fault zones. For the Kyrgyz Tianshan, Palaeogene–Neogene cooling ages are almost exclusively found in close vicinity to major fault zones, while further away from the major structures, 'background' regional Mesozoic cooling ages dominate. For the Siberian Altai-Sayan, latest Cretaceous–early Palaeogene cooling ages were found in the major structures in comparison to the regional Mesozoic cooling ages. For both regions, different processes are required to explain the nature and preservation of the Mesozoic versus Cenozoic cooling signals.

The different mechanisms that induced regional versus localised cooling via fault-reactivation are illustrated in Figs. 4 and 5. Regional slow/moderate cooling signals in combination with the production of significant quantities of detrital sediments in adjacent basins can be explained by denudation as a response to regional uplift and/or base-level drop. Fig. 4 illustrates the relationship between regional cooling and denudation (modified after Wagner and Van den haute, 1992; Summerfield and Brown, 1998). After a period of intense regional tectonic uplift, a rock volume (green cube), initially (time t_0) at ~2.5 km depth with respect to sea level (~90 °C for a 'normal' geothermal gradient), is transported to a depth of ~1.5 km with respect to sea-level at time t_1. The isotherms are passively uplifted along with the rock volume and thus no cooling is registered. As a consequence of the increased relief, denudation of ~1 km of rock sets in. Hence, the mass of the crust reduces and temporary isostatic disequilibrium develops at time t_2. To correct for this unstable situation, isostatic rebound and thermal relaxation takes place at time t_3, which will consequently cool the sample down to ~60 °C in this example. The thermochronometric clocks will register the cooling of the rock volume between time t_1 and time t_3 and, in case of the AFT method, the cooling age will only be frozen in the rock sample when time t_3 has been reached. However, since there can be quite a major time lag between the start and end of the denudation process, the resulting cooling age does not necessarily date the initiation of the tectonic event. Slow denudation and associated exhumation during this time lag allows the thermochronometric clocks to be partially reset as the rocks are thus moving slowly through the so-called partial retention zones (PRZ) associated with each of these clocks. In other words, due to this time lag the resulting cooling age will be registered somewhere between t_1 and t_3, while the tectonic event took place at time t_1. Only when denudation was rapid and extensive enough (largely controlled by climatic conditions or landscape properties such as slope stabilities), the thermochronometric clocks will register the associated cooling phase (e.g. Summerfield and Brown, 1998). However, the response of cooling to regional denudation is often rather slow/moderate, resulting in a wide range of apparent cooling ages, which may explain the large variety in Mesozoic cooling ages within both the Kyrgyz Tianshan and Siberian Altai-Sayan. When denudation rates are very slow, such as within internally drained plateaus or regions with little local slope (e.g. Summerfield and Brown, 1998), older cooling events may be preserved in the thermochronological record of the basement. These stable landscape remnants can be found within active mountain belts such as Central Asia (e.g. Jolivet et al., 2007; De Grave et al., 2011) or Tibet (e.g. Hetzel et al., 2002).

In contrast, Cenozoic cooling in Central Asia is widely modelled as being more rapid and this requires vast quantities of Cenozoic strata in adjacent basins to explain the cooling signals with the mechanism described above. Given that most of the young (Cenozoic) cooling ages are obtained within major fault-zones (currently

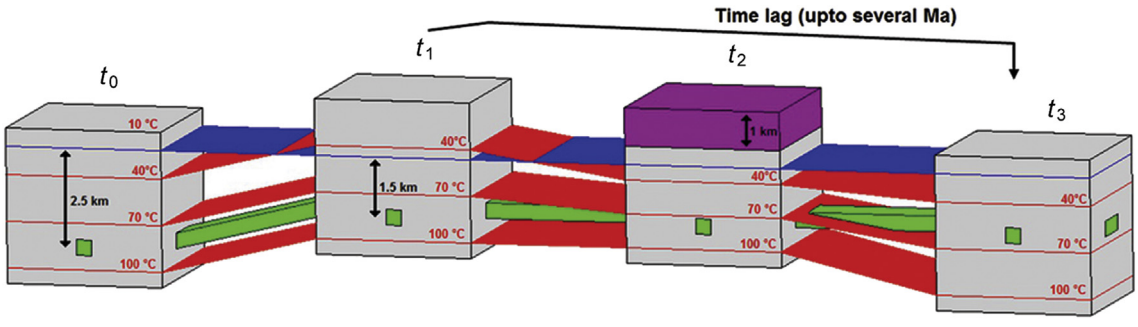

Figure 4. Schematic cartoon, illustrating the relationship between regional cooling and denudation (modified after Wagner and Van den haute, 1992; Summerfield and Brown, 1998). After a period of intense regional tectonic uplift, a rock volume (green cube), initially (time t_0) at ~2.5 km depth with respect to sea level (~90 °C for a 'normal' geothermal gradient), is transported to a depth of ~1.5 km with respect to sea level at time t_1. The isotherms are passively uplifted along with the rock volume and thus no cooling is registered. As a consequence of the increased relief, denudation of ~1 km of rock sets in. Hence, the mass of the crust reduces and temporary isostatic disequilibrium develops at time t_2. To correct for this unstable situation, isostatic rebound and thermal relaxation takes place at time t_3, which will consequently cool the sample down to ~60 °C in this example. The thermochronometric clocks will register the cooling of the rock volume between time t_1 and time t_3 and, in case of the AFT method, the cooling age will only be frozen in the rock sample when time t_3 has been reached. However, since there can be quite a major time lag between t_1 and t_3, the resulting cooling age does not necessarily date the initiation of tectonic uplift. See text for more details.

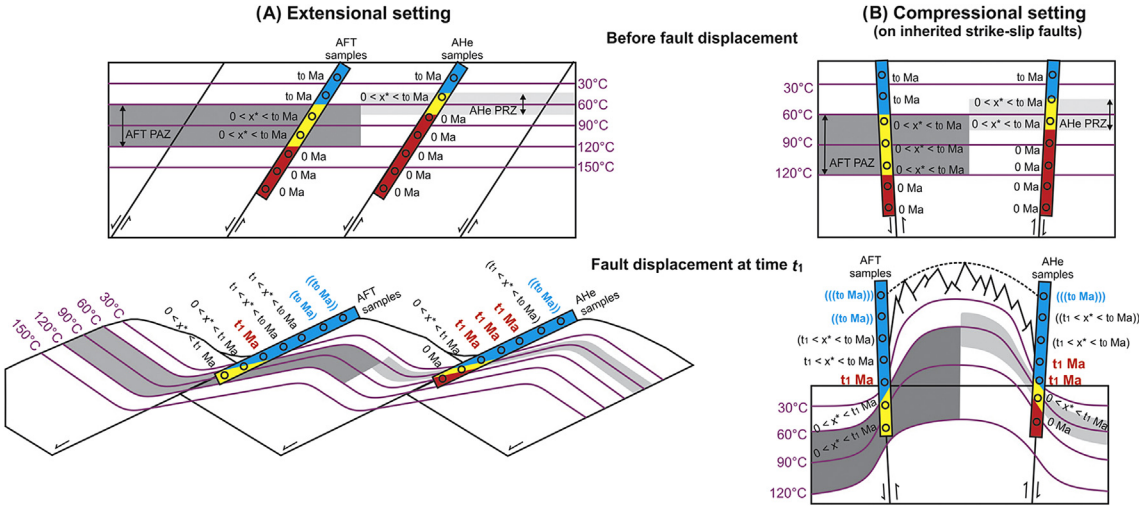

Figure 5. Schematic cartoon, illustrating the relationship between localised cooling and exhumation within fault zones. The model is explained for a stack of normal faults that exhume the footwall during extension (panel A, modified after Stockli et al., 2000; Stockli, 2005), as well as for a stack of strike-slip faults which are reactivated as reverse faults (e.g. Selander et al., 2012) that exhume the hanging wall during compression (panel B). Before fault-induced exhumation occurs, the cooling ages registered along the fault escarpments reflect the thermal structure of the crust. For rocks that are hotter than ~120 °C for the AFT clock and ~75 °C for the AHe clock, cooling is not registered and all previous cooling events are erased (0 Ma; red zone = total reset). Rocks that are colder than ~60 °C for the AFT clock and ~45 °C for the AHe clock record a preserved cooling age t_0 (blue zone = total retention), related with an older cooling event. In between those temperature brackets, both clocks record a meaningless cooling age (yellow zone = partial retention) in between 0 and t_0 Ma. The extent of this yellow zone of partial retention depends on the local geothermal gradient. During faulting at time t_1, the footwall (panel A) or hanging wall (panel B) rocks become quickly exposed in the fault escarpment, cooling nearly the entire rock-sequence into the total retention zone (blue zone in Fig. 5). As a result, rocks that were originally in the total reset (red) zone are exhumed rapidly through the partial retention zone (yellow), into the total retention zone (blue) and will thus record the timing of faulting (t_1). Rocks that were already in the total retention zone before the faulting event will maintain their original cooling age (t_0). In a vertical section, the lowermost samples will thus likely date the timing of faulting, while those near the top will yield either a meaningless PRZ age or the timing of an older exhumation event (depending on the preservation potential of the upper part of the fault escarpment). Given that the geothermal gradient is generally higher within active faults than in the surrounding crust, the extent of meaningless PRZ data is likely relatively small within exposed fault escarpments. See text for more details.

reactivated as large-scale strike-slip and thrust faults), it is suggested that fault induced deformation is responsible for fast exhumation and associated cooling (e.g. Glorie et al., 2011a). Both the Cenozoic Kyrgyz Tianshan and Siberian Altai-Sayan largely exhumed as a response to crustal shortening. For the Kyrgyz Tianshan, the mountain ranges are thought to be exhumed 'out-of-sequence' within a large-scale flower-structure (e.g. De Grave et al., 2013; Macaulay et al., 2014), exposing 'squeezed-out' basement-cored uplifts (hanging wall rocks) along inherited strike-slip faults. These inherited strike-slip faults became reactivated as steeply dipping reverse faults, often exposing steep fault escarpments (e.g. Selander et al., 2012). Similarly for the Siberian Altai-Sayan, the present relief is largely controlled by the reactivation of suture-shear zones as major thrust or transpressive systems (e.g. Dehandschutter et al., 2002; Thomas et al., 2002; Glorie et al., 2012a).

The relationship between rapid cooling and exhumation via faulting is illustrated in the cartoon in Fig. 5 where a stack of lithospheric-scale faults divide the crust into a number of fault-bounded blocks. The mechanism is explained for a stack of normal faults that exhume the footwall during extension (panel A, modified after Stockli et al., 2000; Stockli, 2005), as well as for a stack of strike-slip faults which are reactivated as reverse faults that exhume the hanging wall during compression (panel B). Latter model is more appropriate for fault reactivation in Central Asia (e.g. Selander et al., 2012) than the published model for extensional fault-exhumation; however both mechanisms are very similar. Both models quickly expose a vertical section through the crust without the need of major associated denudation and production of detrital deposits.

Before fault-induced exhumation occurs, the cooling ages registered along the fault escarpments reflect the thermal structure of the crust. For rocks that are hotter than ~120 °C for the AFT clock and ~75 °C for the AHe clock, cooling is not registered and all previous cooling events are erased (0 Ma; red zone = total reset). Rocks that are colder than ~60 °C for the AFT clock and ~45 °C for the AHe clock record a preserved cooling age t_0 (blue zone = total retention), related with an older cooling event. In between those temperature brackets, both clocks record a meaningless cooling age (partial retention zone = yellow zone in Fig. 5) in between 0 and t_0 Ma. The extent of this yellow zone of partial retention depends on the local geothermal gradient. During faulting at time t_1, the footwall (hanging wall for compressional settings) rocks become quickly exposed in the fault escarpment, cooling nearly the entire rock-sequence into the total retention zone (blue zone in Fig. 5). As a result, rocks that were originally in the total reset (red) zone are exhumed rapidly through the partial retention zone (yellow), into the total retention zone (blue) and will thus record the timing of faulting (t_1). Rocks that were already in the total retention zone before the faulting event will maintain their original cooling age (t_0). However, the newly created topography becomes quickly subjected to denudation/erosion and it is therefore unlikely that the uppermost samples in the fault escarpments are preserved (ages within brackets in Fig. 5). The rate of erosion and hence the preservation potential of these ages is largely controlled by local external conditions such as the local climate, relief (slope stability) and lithology (e.g. Summerfield and Brown, 1998). In specific conditions as discussed above, the older relief and their associated inherited cooling ages may be preserved.

In addition, some samples in the fault escarpment will register a meaningless mixing age between the timing of faulting and the older event. These are the samples that came out of the exhumed partial retention zone. It is therefore necessary to (1) obtain samples from the largest possible range of intact pre-displaced palaeodepths (e.g. Stockli et al., 2000) and/or (2) to apply multiple thermochronometers on the same fault zone in order to find the

sample(s) that date the timing of faulting. These samples will, if exposed, likely come from the bottom section of the escarpment as samples from below the exhumed partial retention zones are invariant in age and directly date the timing of inception of footwall/hanging wall cooling and faulting (e.g. Stockli et al., 2000). Note that active faults are often regarded as 'heat pumps', characterised by extremely high local geothermal gradients during faulting (e.g. Meneghini et al., 2012). This effect is largely neglected in the cartoons in Fig. 5. Although the effect of this heat-pumping on thermochronological data in fault zones is not well understood, it may be significant as the exposure to the partial retention zone during faulting may be significantly shorter as a result of these extreme local geothermal conditions. In other words, the section of meaningless mixing ages within these fault zones is generally much smaller than in a slowly cooled terrane.

It is thus of vital importance to understand the basement architecture in order to comment on the geographical distribution of thermochronometric data across mountain ranges. Tectonically-induced far-field stresses will likely first affect the major fault zones which act as zones of weakness within the continental interior. Resulting fault reactivations can induce localised cooling of the exposed basement and will therefore rapidly reset the thermochronometric clocks (Fig. 4). This process would induce apparent anomalously young cooling ages in the fault escarpments. When these cooling ages are well-constrained, preferably by multiple independent thermochronometric clocks, they hold key-information on the deformation history of the study area and therefore should not be neglected.

In the case of the Kyrgyz Tianshan, Macaulay et al. (2014) identified 'anomalous ages' in the AFT data both north and south of Issyk-kul lake as they appeared to be too young compared to other data in the same sampling transects. These authors therefore assumed that 'these samples had analytical problems which lead to erroneous ages'. These 'anomalously' young ages were obtained on basement samples taken in the exposed escarpments of the Karakung-Almaty (KAF) and Main Terskey (MTF) faults (~23 and ~5 Ma samples in profile A–A′, Fig. 2). The ~5 Ma AFT cooling age in the Main Terskey fault is debatable as it is not reproduced by other thermochronometric clocks. However, given that the AFT age was consistent for 60 individual apatite crystals (De Grave et al., 2013) it is unlikely affected by analytical problems. The ~23 Ma AFT age in the KAF (near the Kazakh-Kyrgyz border) is confirmed by its ~15 Ma AHe age, indicating that an event of rapid Neogene cooling was registered in the fault-escarpment (Fig. 2). More recently ~17–10 Ma AFT ages were obtained for samples within the adjacent Zaili Fault escarpment (De Pelsmaeker et al., 2015). These data indicate that both the KAF and ZF were reactivated during the Neogene, similar as other major structures within the Kyrgyz Tianshan (e.g. the South Tianshan suture-shear zone; e.g. Glorie et al., 2011a). This Neogene fault activity is not surprising given that both faults are located within a zone of high seismic activity (e.g. Torizin et al., 2009; De Pelsmaeker et al., 2015). The southern slopes of the Kungey Range are not within this zone of high seismic activity and more likely form part of a tilted palaeo-surface, registering only the regional Mesozoic cooling (Fig. 2; De Grave et al., 2013).

As mentioned above, apatite fission track data alone are not necessarily good estimates of the timing of exhumation. Especially in slowly cooled terranes, these apparent AFT ages are often meaningless and merely reflect an exhumed part of an old partial retention zone (as discussed above). Therefore additional data is required to constrain the rate of cooling (fast versus slow) and to assess if the AFT age can provide a meaningful estimate on the timing of initiation of cooling/exhumation. This can be done using (1) thermal history modelling based on AFT length distributions as proxy for the cooling rate; (2) with age-elevation profiles using the slope in age-elevation plots as a proxy for the cooling rate; (3) with multiple thermochronometric clocks using the timing of passing through the different closure temperatures as a proxy for the cooling rate, or with a combination of these three methods. Using age-elevation profiles alone however is often hazardous as a consequence of low temperature isotherm compression in (rapidly) exhumed terranes (e.g. Valla et al., 2010; van der Beek et al., 2010) and it is therefore preferably combined with one of the other two methods to deduct the timing of initiation of cooling.

In order to assess the rate of regional cooling/exhumation, all of these three methods can be used; however thermal history modelling is often the preferred method. The reduction in fission track lengths is a function of the rate of cooling through the apatite partial annealing zone (e.g. Wagner and Van den haute, 1992) which can be modelled together with the apparent fission track age to constrain the timing of cooling/exhumation (e.g. Ketcham, 2005). Age-elevation plots are often used as well to assess how fast the samples cooled through the partial retention zone and to identify a so-called 'break-in-slope' which indicates the timing of initiation of cooling (e.g. Gleadow and Fitzgerald, 1987; Wagner and Van den haute, 1992; De Grave et al., 2011). In the case of young fault reactivations, the thermal history modelling is often hindered by a lack of confined fission tracks in the samples. In this case, multi-method thermochronology is the preferred method to assess the timing of fault-induced cooling. When these different clocks, that are sensitive to different closure temperatures (described above), yield a similar cooling age, this age represents the timing of an episode of fast cooling, which can often be linked to rapid exhumation as a response to a distinctive tectonic event (e.g. Summerfield and Brown, 1998; Moore and England, 2001). In the context of Central Asia, which is currently an active intra-continental mountain belt, these cooling events are thought to represent far-field effects of the tectonic activity at the plate margins (e.g. De Grave et al., 2007).

4. Discussion and comparisons

4.1. Timing of exhumation of the Kyrgyz Tianshan and Siberian Altai-Sayan

In order to assess the timing of cooling as response to exhumation within the Kyrgyz Tianshan and Siberian Altai-Sayan, all available thermochronological data are plotted in a time-temperature diagram for both regions (Fig. 6). Representative thermal history models, which provide an estimate of the relative cooling rates associated with each cooling event, are indicated as well. Meaningful age-elevation profiles are provided as insets in Figs. 2 and 3 to further constrain the relative cooling rates.

4.1.1. Triassic–early Jurassic

In some specific locations within the Kyrgyz Tianshan, Triassic–early Jurassic cooling was recorded. Most notable is the Song-kul plateau (Fig. 2), where Triassic–early Jurassic TFT, AFT and AHe ages were obtained. Post early Mesozoic denudation of the Song-kul basement was limited and uplift of the entire basin created an internally drained plateau, allowing preservation of these old TFT and AFT basement ages. This is attested to by the fact that the upper section of exhumed fossil AFT and TFT partial annealing zones (PAZ) are preserved in the basin-vergent mountain slopes surrounding the Song-kul plateau. The current morphology of the Song-kul block was hence already established after the early Mesozoic cooling event (discussed further below) (De Grave et al., 2011). Both the age-elevation profiles (Fig. 2) as well as representative thermal history models (Fig. 6) indicate that

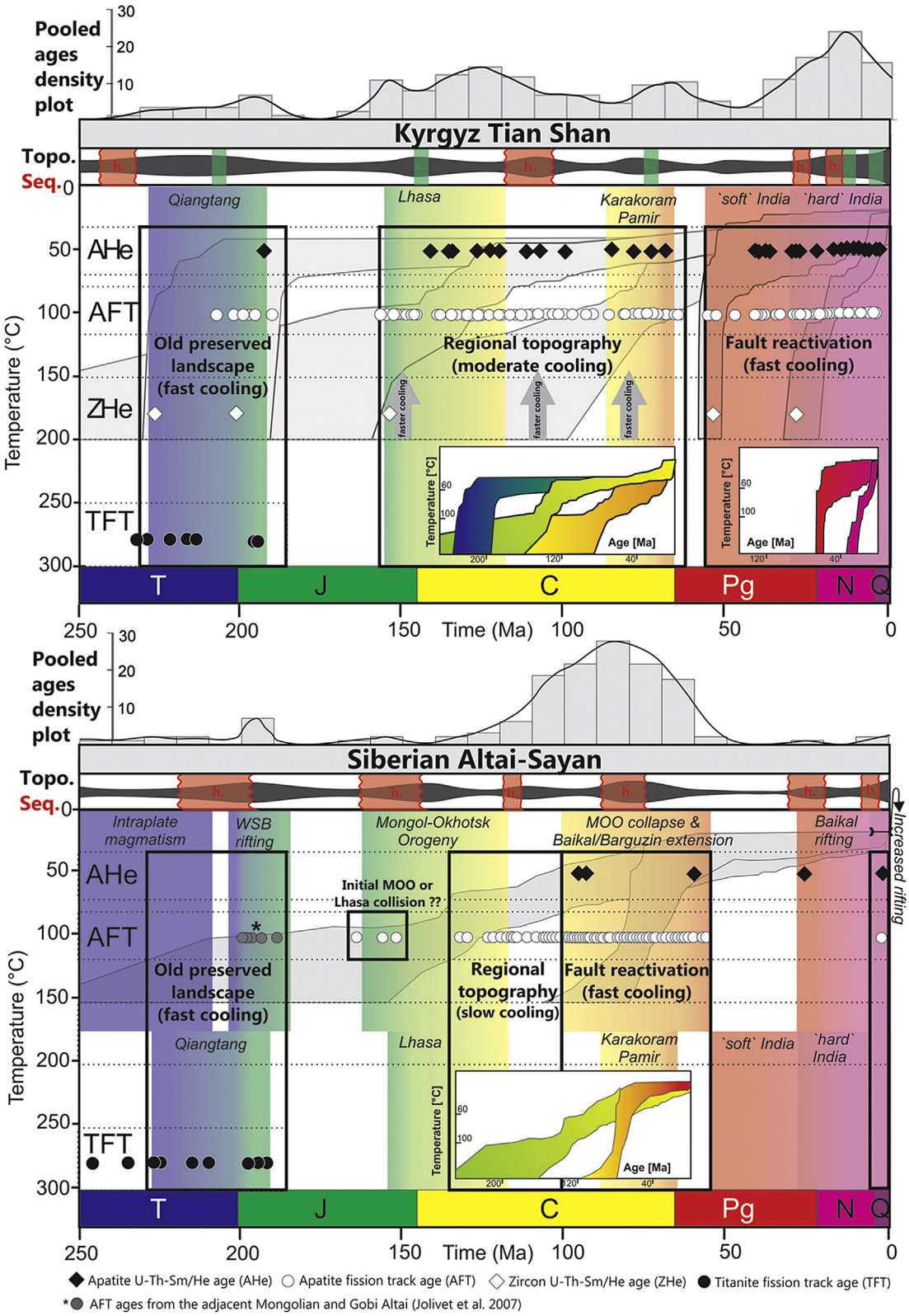

Figure 6. Summary of all available apatite and titanite fission track (AFT/TFT) and apatite and zircon U-Th-Sm/He (AHe/ZHe) data in time-temperature space for the Kyrgyz Tianshan (above) and the Siberian Altai-Sayan (below). Representative cooling models are indicated as well as an estimate of the relative cooling rates. The thermochronometric data is compared with the timing of the main collisional events at the distant plate-margins in order to speculate on the driving forces of the cooling pulses. Seq. refers to additional sedimentary constraints with h. = hiatus, c. = (alluvial) conglomerates, based on sedimentological data from the Tarim (Dumitru et al., 2001 and references therein), Chu (Bullen et al., 2001 and references therein) and Issyk-kul basins (Cobbold et al., 1994) for the Tianshan and from the Kuznetsk (Davies et al., 2010), West-Siberian (Vyssotski et al., 2006) and Chuya basins (Buslov et al., 1999). Using the thermochronometric and sedimentological data, estimates were made of the topographic evolution of the Kyrgyz Tianshan and Siberian Altai-Sayan (Topo.). For the Tianshan, these estimates compare well with Jolivet et al. (2013). Pooled age-density plots are shown as well which depict the main cooling pulses associated with the regional and local relief expressions. Refer to Figs. 2 and 3 for references to the original data.

the preserved Triassic–early Jurassic cooling was rapid and induced significant exhumation at that time. Late Triassic–Jurassic sediments are arguably not highly abundant within the Kyrgyz Tianshan compared to the early–middle Triassic and Cretaceous sedimentary record and are limited to restricted sequences in e.g. the Ferghana Basin (e.g. Sanders and Long, 1994). Presumably, most of the Triassic–Jurassic sedimentary record has been reworked by subsequent exhumation events. The Triassic–early Jurassic cooling coincides with the occurrence of a major alluvial conglomerate unit (~215 Ma) in the stratigraphic record of the adjacent Tarim Basin (Fig. 1; Dumitru et al., 2001 and references therein) and Kuqa Basin (Jolivet et al., 2013 and references therein). Furthermore, Triassic cooling ages were also found within detrital apatites from Meso–Cenozoic sediments in e.g. the Chu and Ferghana basins, indicating that a record of the rapid Triassic–early Jurassic exhumation is preserved within the intramontane basin sediments as well (Fig. 2; Bullen et al., 2001, 2003; De Grave et al., 2012).

Within the Siberian Altai-Sayan, Permian–early Jurassic TFT ages were obtained (Figs. 3 and 6) which show a shallow trend in the age-elevation profile (Fig. 3). These ages are indicative for slow cooling, presumably related with post-magmatic cooling of the Permian–Triassic intra-plate intrusions in the Siberian Altai basement (Glorie et al., 2011b, 2012a). Intrusions sampled in close vicinity of the CTUSS however yield significantly younger, late Triassic–early Jurassic (~240–195 Ma) TFT ages and show a trend of rapid cooling in age-elevation profile (Figs. 3 and 6). Hence, the Siberian Altai was affected by a period of rapid late Triassic–early Jurassic exhumation and fault reactivation (Glorie et al., 2012a), similar as described for the Kyrgyz Tianshan. However, this cooling event is not preserved in the AFT data for the Siberian Altai. Late Triassic–early Jurassic AFT ages are only found in specific locations within the Altai-Sayan such as the preserved old relief of the Gobi and Mongolian Altai (Jolivet et al., 2007; Vassallo et al., 2007). This Triassic – late Jurassic basement cooling corresponds with a sedimentary hiatus in the West-Siberian and Kuznetsk basins, to the north of our study area (Fig. 6). Underneath this unconformity, signs of compressive deformation were observed in the sediments, indicating that an important late Triassic–early Jurassic orogen must have existed within the Siberian Altai-Sayan (e.g. Le Heron et al., 2008; Davies et al., 2010).

4.1.2. Late Jurassic–late Cretaceous/early Palaeogene

During most of the Jurassic (~180–160 Ma), both the Kyrgyz Tianshan and Siberian Altai experienced a period of tectonic quiescence, resulting in extensive peneplanation of the Triassic–early Jurassic relief (e.g. Jolivet et al., 2007, 2013). Remnants of an associated planation surface are preserved in several locations within the Tianshan (e.g. Jolivet et al., 2010). The Kyrgyz Tianshan experienced renewed cooling since the late Jurassic (~160 Ma) which coincides with the widespread occurrence of conglomerate deposits in the adjacent Tarim and Junggar basins (Jolivet et al., 2013 and references therein). As shown in Fig. 6, this cooling phase seems to be more or less continuous from the late Jurassic until the late Cretaceous–early Palaeogene. Representative thermal history models (Fig. 6) indeed show that the middle–late Mesozoic was mainly characterised by a period of protracted slow cooling. Nevertheless, three phases of accelerated cooling can be identified within this time period. A first pulse is defined by ZHe and AFT ages at ~160–145 Ma and corresponds to the occurrence of a major alluvial conglomerate in the sedimentary record of the Tarim and Junggar basins (Jolivet et al., 2013, Fig. 6). This cooling pulse likely induced new relief in the Kyrgyz Tianshan which is preserved in several locations (pale green ages in Fig. 2). The large spread in ~145–120 Ma AFT and AHe data likely reflects slow cooling and prolonged residence in the AFT and AHe partial retention zones. AFT data seems to be more densely concentrated around ~120–95 Ma which corresponds well with a major hiatus in the sedimentary record of the Tarim Basin (Fig. 6, Dumitru et al., 2001 and references therein). For several samples, similar ~120–90 Ma AFT and AHe ages were obtained and accelerated cooling was observed in associated thermal history models. These 'middle' Cretaceous cooling ages are in fact the most common age population within the Kyrgyz Tianshan. From ~90–75 Ma, AFT and especially AHe data is scarcer, suggesting steady slow cooling or tectonic quiescence. A subsequent third pulse of more rapid cooling/exhumation is evident by a dense cluster of AFT data at ~75–60 Ma and increasing cooling rates in thermal history models (Fig. 6; De Grave et al., 2013). Latter pulse coincides with the occurrence of a new alluvial conglomerate in the Tarim Basin (Dumitru et al., 2001). These coarse, molasse-type sediments and stratigraphic hiatuses from the same periods are widespread in intramontane depressions within the Tianshan orogen as well (e.g. the Issyk-kul Basin in Kyrgyzstan; Cobbold et al., 1994).

Late Mesozoic cooling within the Altai-Sayan starts in the late Jurassic as shown by limited AFT age data. However, more than 90% of all obtained AFT and AHe ages are Cretaceous–early Palaeogene, suggesting that most of the present-day regional Altai-Sayan landscape is largely a relic of a late Mesozoic relief (e.g. Glorie et al., 2012). In specific locations this Mesozoic relief has been overprinted by subsequent events, however associated denudation was generally not extensive enough to reset the thermochronometric clocks during these later events (discussed further below). Late Jurassic cooling AFT ages correspond well with a large stratigraphic hiatus within the adjacent Kuznetsk Basin (e.g. Davies et al., 2010, Fig. 6), suggesting that the Altai-Sayan exhumed at that time. Abundant AFT age data suggest nearly continuous cooling throughout the Cretaceous–early Palaeogene (Fig. 6), however, as discussed above, two different trends can be recognised within associated age-elevation profiles (Fig. 3). A slow cooling trend can be observed representing protracted residence within the partial annealing zone during the early Cretaceous. Associated thermal history profiles indeed show slow cooling at that time (e.g. Glorie et al., 2012; Fig. 6). Hence, the middle Cretaceous (~130–100 Ma) cooling likely induced only minor relief in the Siberian Altai-Sayan, which corresponds with the occurrence of several minor stratigraphic hiatuses (during the Barremian–early Albian) in the eastern part of the West-Siberian basin (Vyssotski et al., 2006). Cooling rates increase since ~100–90 Ma as indicated by both thermal history profiles (Fig. 6) as well as by a steepening in age-elevation trends and mimicking AFT and AHe ages (Fig. 3). Interestingly, the late Cretaceous–early Palaeogene cooling ages were only found within large-scale fault zones, indicating that the late Cretaceous–early Palaeogene cooling and exhumation is largely structurally controlled (Glorie et al., 2012; De Grave et al., 2014; Fig. 3). As a result, significant relief was created during the late Cretaceous–early Palaeogene and most of this relief is still preserved within the Altai-Sayan. This event did not produce vast amounts of sedimentary detritus in the adjacent basins as associated denudation was only localised within the fault escarpments, which is conform with the fault-induced exhumation model discussed above. The timing of fault reactivation is constrained to ~95–75 Ma (depending on the exact location) by the age-elevation profiles (Fig 3), cooling history models (Fig. 6) and a major sedimentary hiatus (during the late Campanian) within the West-Siberian Basin (Vyssotski et al., 2006).

4.1.3. Palaeogene–Neogene

For the Kyrgyz Tianshan, a period of renewed fast cooling is observed in the thermochronological data (AFT, ZHe, AHe) during the early Palaeogene (~55–45 Ma). In fact, most of the published

thermochronological data for the Kyrgyz Tianshan is Cenozoic in age (although this is mostly biased by sampling strategies). These cooling ages were only found in close vicinity to major fault zones, indicating that Palaeogene cooling is mainly controlled by fault reactivations (Fig. 2). Jolivet et al. (2010) recognised fault-induced reactivation focussed on large inherited structures around ~60 Ma in the Chinese Tianshan as well, indicating that Palaeogene fault reactivation occurred throughout the entire Tianshan. This fast cooling event clearly affected only the weaker fault zones in the Tianshan edifice, while in more rigid parts, Mesozoic cooling ages are preserved. Similar as discussed above, these fault reactivations are not associated with large-scale denudation and therefore, the Palaeogene sedimentary record is generally rather restricted in adjacent foreland and intramontane basins. Both the thermal history models and the AFT, ZHe and AHe ages indicate that cooling was rapid at that time (Fig. 6; e.g. Glorie et al., 2011).

Most of the Cenozoic cooling ages obtained within the major fault zones, however, are late Palaeogene–Neogene. Oligocene–Pliocene (~33–3 Ma) AFT, AHe and even ZHe reset ages were obtained within the faulted basement and associated thermal history models, show that this period was characterised by fast cooling (Fig. 6). The timing of onset of accelerated cooling cannot easily be derived based on thermochronological data, given that exposed fault escarpments will likely preserve an exhumed section of the partial retention zone associated with each thermochronological clock (as discussed above). Combining similar cooling ages from different thermochronometric methods with rapid cooling steps in the thermal history models and the occurrence of sedimentary hiatuses and alluvial gravels (Fig. 6), it is suggested that the onset of the modern Kyrgyz Tianshan orogeny occurred during the Oligocene–early Miocene (~33–22 Ma) with an apparent intensification in the late Miocene (~12–8 Ma) and the Plio–Pleistocene (<5 Ma). The specific location of these cooling ages within major fault zones demonstrates that the deformation associated with the modern mountain building has not migrated steadily into all parts of the Kyrgyz Tianshan, but remained tectonically confined to pre-existing basement structures. The pre-existing basement architecture has therefore a dominant influence on the intracontinental deformation within the Tianshan and the data presented here, in our opinion, are a clear expression of this.

The extent of both fault reactivation events and associated mountain ridge uplift varies along strike (e.g. Glorie et al., 2011; Macaulay et al., 2014). This can be demonstrated by the variation in cooling ages (ZHe, AFT, AHe) along strike of the South Tianshan Suture (STSS). For both the eastern (Inylchek region) and the western (Atbashi region) along the STSS, mainly Neogene (~20–5 Ma) cooling ages were obtained, while within the centre of this fault zone, only early Palaeogene cooling ages are preserved (Glorie et al., 2011; Fig. 2).

For the Siberian Altai-Sayan, only limited Cenozoic cooling ages were obtained, indicating that most of the modern relief is a relic of the Mesozoic landscape. Steeper mountains near major fault zones have undergone more recent uplift, which is in most cases not reflected in the thermochronological data. The lack of Cenozoic cooling ages is likely due to insufficient denudation to reset the thermochronometric clocks. Limited early Neogene AFT ages were likely sampled from within the preserved partial retention zone and are thus probably meaningless. They nevertheless coincide with a stratigraphic hiatus and subsequent conglomerates and coarse sand deposits in the Kurai-Chuya Basin, which may indicate that the Altai was being uplifted and exhumed at that time (e.g. Delvaux et al., 1995). Late Pliocene–Pleistocene (~3–1 Ma) AFT and AHe ages are thought to represent more reliable cooling ages and may therefore indicate the timing of recent fault reactivation (Glorie et al., 2012; De Grave et al., 2014). These Plio-Pleistocene cooling ages were only obtained at specific locations along the Charysh-Terekta-Ulagan-Sayan and West Sayan fault zone (Fig. 3). As explained above, the fault reactivation model does not require large quantities of associated Plio–Pleistocene detrital deposits in adjacent basins, however, the Plio–Pleistocene sedimentary record in adjacent sedimentary basins is characterised by a sedimentary hiatus at that time (e.g. Buslov et al., 1999). Structural analysis in the Sayan Mountains confirms that inherited basement structures were reactivated during the Plio–Pleistocene (Arzhannikova et al., 2011). Moreover, tectonic activity within these fault zones is still very active today as attested by the occurrence of historical and recent earthquakes along the northern margin of the Chuya basin for example (e.g. Lunina et al., 2008).

4.2. Linking intracontinental deformation with plate-margin processes

The thermochronological datasets of both the Kygyz Tianshan and the Siberian Altai-Sayan record several cooling events during the Meso–Cenozoic. These cooling pulses reflect increased regional denudation of the landscape or local fault reactivations as discussed above. Throughout the Meso–Cenozoic, the Eurasian continent was subjected to several phases of compression related to the convergence and collision of (micro-)continental blocks or island-arcs at the southern plate margin. In addition, processes such as orogenic collapse, slab-break off and rifting/extension may have induced deformation in the Eurasian interior as well. This section aims to contrast the punctuated cooling history, captured within the thermochronological data, with the documented tectonic history of the Eurasian plate in order to speculate on the causes of the punctuated intracontinental deformation within Central Asia.

4.2.1. Triassic–early Jurassic

Preserved old landscape relics within both the Kyrgyz Tianshan and the Siberian Altai record a Triassic–late Jurassic cooling event. This basement cooling event is coeval with the onset of so-called Cimmerian collisions on the southern Eurasian margin. During the middle Triassic, the Palaeo-Tethys Ocean started to close, resulting in the accretion of several Cimmerian tectonic units (e.g. Golonka, 2004). In this respect, the Cimmerian Qiangtang block collided with the Kunlun terrane at the southern Eurasian margin during the middle to late Triassic (~230–190 Ma). This collision occurred along the Jinsha suture south of Tarim, in present-day Tibet and the Pamirs (e.g. Ratschbacher et al., 2003; Schwab et al., 2004; Zhai et al., 2011). It is thought that the Qiangtang collision with Eurasia induced fault reactivations and basement exhumation within Central Asia (Fig. 6). This is especially the case for the Kyrgyz Tianshan which had a proximal location to the collision zone (e.g. De Grave et al., 2011, 2013). In addition, the Triassic collision of a related Cimmerian unit, the Turan plate to the west of the Pamir block (e.g. Alexeiev et al., 2009), and extension and subsidence in the Tarim Basin (e.g. Zhang et al., 2010) may also have played a role in the early Mesozoic reactivation in the Kyrgyz Tianshan.

The role of the early Cimmerian collision of the Qiangtang (and Turan) blocks to Eurasia with respect to the Triassic–early Jurassic exhumation pulse in the Siberian Altai-Sayan is not well understood. Due to the more distal location of the Siberian Altai-Sayan with respect to the early Mesozoic Eurasian plate-margin, the compressional stresses associated with the Qiangtang collision had to propagate further into the continental interior in order to affect the Siberian Altai-Sayan. However, during the Triassic–early Jurassic, the West Siberian basin started to subside, creating a base-level drop to the northwest of the Siberian Altai-Sayan (Allen et al., 2006; Vyssotski et al., 2006). In fact, most of Siberia was affected by

extensional tectonics at that time, which is likely related with a pulling effect of the Mongol-Okhotsk Ocean which started to subduct at the eastern margin of Siberia (e.g. Golonka et al., 2003). This is further underscored by palaeomagnetic data on sediments from the Taimyr fold belt in Arctic Siberia, revealing that middle–late Triassic (~230–220 Ma) deformation occurred in this region (Torsvik and Andersen, 2002). It is hence likely that the prevailing extensional deformation during the Triassic affected the Siberian Altai-Sayan as well.

Alternatively, the older Triassic (early–middle Triassic) cooling ages obtained for the Kyrgyz Tianshan and especially for the Altai-Sayan could be linked with the final amalgamation of the Central Asion Orogenic Belt, prior to its reactivation. Xiao et al. (2013) suggests that the terminal amalgamation (including orogenic collages in the Chinese Tianshan) occurred during the middle Triassic, which coincides with the locally preserved Triassic cooling signal in certain landscape features (e.g. De Grave et al., 2011) and within fault zones (e.g. Glorie et al., 2011a, 2012a).

4.2.2. Late Jurassic–late Cretaceous/early Palaeogene

Abundant thermochronological data indicate that a late Mesozoic Tianshan orogen was built as a response to the punctuated accretion of several Cimmerian blocks to the Mesozoic Eurasian margin. In contrast to the early Mesozoic event that is only locally preserved within the Kyrgyz Tianshan and in the intramontane Kyrgyz Tianshan detrital record, this late Mesozoic event affected the entire Tianshan, across terrane boundaries. As discussed above, three main pulses of late Mesozoic regional cooling can be distinguished which can be linked with distinct tectonic events at the southern Eurasian plate margin (Fig. 6). The first (late Jurassic–early Cretaceous, ~160–145 Ma) cooling pulse is only registered and/or preserved in a handful of samples. Although the significance of this cooling pulse is debatable, it is coeval with the late Jurassic–early Cretaceous (~150–120 Ma) collision of the Cimmerian Lhasa Block with Eurasia (Kapp et al., 2007). It is thought that this collision exerted distant tectonic effects onto the Kyrgyz Tianshan (e.g. De Grave et al., 2013). However, this interpretation is debatable since this collision only had minor influence on the cooling and exhumation of eastern Tibet and Qaidam, more close to the collision zone (e.g. Jolivet et al., 2001, 2013; Roger et al., 2010). The second (mid-Cretaceous, ~120–95 Ma) cooling pulse is more extensively preserved throughout the Kyrgyz Tianshan and cannot easily be linked to distant compressional tectonic forces. Several recent studies document the occurrence of coeval ~110 Ma bimodal volcanic rocks within northern and Central Lhasa, just south of the Kyrgyz Tianshan. These rocks are thought to be formed in an extensional setting related with slab break-off of the subducting Bangong–Nujiang Tethyan Ocean lithosphere (e.g. Sui et al., 2013; Chen et al., 2014). The mid-Cretaceous cooling event within the Kyrgyz Tianshan can therefore be interpreted as an isostatic response to the slab-break-off model. However, more data is required to confirm this hypothesis. The third (late Cretaceous–early Palaeogene, ~75–60 Ma) cooling pulse occurred largely coevally with the collision of the Kohistan-Dras island-arc (Treloar et al., 1996) and the Karakoram Block to Eurasia (~80–70 Ma; Schwab et al., 2004). Similar as discussed for the collisions of the Qiangtang and Lhasa terranes to Eurasia, the Kohistan-Dras and Karakoram collisions may have induced exhumation and cooling within the Kyrgyz Tianshan (e.g. De Grave et al., 2013).

Within the Siberian Altai-Sayan, few late Jurassic AFT ages are locally preserved on the summits of the current landscape. Given that the Lhasa collision seemed to have had only a minor effect on the proximal Kyrgyz Tianshan, it is unlikely that this collision had any effect at all on the Siberian Altai-Sayan. Similar ages were also found in Gobi Altai (Vassallo et al., 2007) and on the margins of the Baikal rift (van der Beek et al., 1996; Jolivet et al., 2009), to the east of the Siberian Altai-Sayan and it is therefore suggested that this cooling signal can be related with the late Jurassic initiation of the Mongol-Okhotsk Orogeny at the eastern plate margin (present-day co-ordinates) (Fig. 6; Delvaux et al., 1995; Cogné et al., 2005; Jolivet et al., 2009). The early–mid Cretaceous (~130–100 Ma) cooling signal probably reflects a protracted residence within the partial annealing zone (as discussed above) and is therefore likely not significant. The associated slow cooling may however reflect a dynamic topographic response to either increased loading on the crust from the growing Mongol-Okhotsk Orogen or the slab break-off model described above. Cooling rates intensified since ~100–90 Ma when large-scale fault reactivation took place within the Siberian Altai-Sayan. The origin of this deformation event is not clear, however, it seems to have occurred coevally with the initiation of extensional tectonics in the southern Baikal rift zone and the Barguzin Basin (Fig. 6; Tsekhovsky and Leonov, 2007; Jolivet et al., 2009). The cause for this intracontinental extension is debatable itself, however it has been suggested that this may be a tectonic response to orogenic collapse of the Mongol-Okhotsk belt (Jolivet et al., 2009). The ~100–90 Ma cooling pulse has been detected in several adjacent locations to the Siberian Altai-Sayan, e.g. along the Irtysh fault in both the Chinese (Yuan et al., 2006) and Kazakh (Rudny) Altai (Glorie et al., 2012b), on the faulted southern margin of Lake Baikal (Jolivet et al., 2009) and along the East Gobi fault zone in southeastern Mongolia (Webb and Johnson, 2006), suggesting that fault reactivations related with extensional tectonics were prevalent throughout most of northern Central Asia at that time.

4.2.3. Palaeogene–early Neogene

In close vicinity of major fault zones within the Kyrgyz Tianshan, rapid early Palaeogene (~55–45 Ma) cooling is observed in the thermochronological data. This fast cooling event clearly affected only the weaker fault zones in the Tianshan edifice, while in more rigid parts, Mesozoic cooling ages are preserved and widespread peneplanation occurred during this period. The driving force for this exhumation phase, focused on the pre-existing basement structures, is still debated but most likely it is a result of the accretion an island-arc system the Eurasian (Tethyan) margin and the associated pronounced northwards thrusting of the Pamir nappes (e.g. Aitchison et al., 2007). In a similar way, Van Hinsbergen et al. (2012) described this event as the so-called 'soft' collision of 'Greater' India with Eurasia, which likely represents the accretion of a peripheral intra-oceanic island-arc system at the northern Indian margin to Eurasia. Aitchison et al. (2000, 2007) argued that this island-arc system is different from the Kohistan-Dras arc described above and represents an entirely separate intra-oceanic island-arc system with correlative ophiolitic suites in the Ladakh region (e.g. the Spong arc). Following Mahéo et al. (2006), this peripheral island-arc system could have been the so-called South Ladakh arc which is thought to have accreted onto the Eurasian margin around ~65–55 Ma. We use this name for the early Cenozoic arc at the southern Eurasian margin (fragmented along the Yarlung Tsangpo suture) in further discussion.

In addition, distant tectonic forces at the southwestern Eurasian margin may have contributed to the Palaeogene deformation and associated exhumation within the Tianshan as well. The occurrence of abundant Palaeocene–Eocene continental arc magmatism (known as the Palaeogene 'flare-up') and Eocene metamorphic core complexes across Iran suggests that this region was under extension during the Palaeogene, which was likely driven by slab retreat and rollback of the subducting Neo-Tethys Ocean (Agard et al., 2011; Verdel et al., 2011; Chiu et al., 2013). Both these extensional forces from the southwest, related with the geodynamic evolution of the Neo-Tethys, and the compressional forces from the southeast,

related with the accretion of an island-arc (the South Ladakh arc?) to Eurasia, may have propagated towards southern Central Asia, inducing reactivations of inherited fault systems within the Kyrgyz Tianshan. Others suggested that the fault reactivations are more likely a far-field effect of the closure of the Mongol-Okhotsk Ocean to the northeast of the Kyrgyz Tianshan (e.g. Wang et al., 2008; Jolivet et al., 2010, 2013). Although this possibility cannot be ruled out based on the discussed datasets, we prefer the more proximal plate-margin processes discussed above as the main contributors for the Palaeogene Tianshan reactivation.

Abundant late Palaeogene–Neogene thermochronological data testify that neotectonic activity is recorded in the major fault zones within the crystalline basement of the Kyrgyz Tianshan which are presumably linked with renewed tectonic reactivation as a far-field effect of the India-Eurasia collision. The data presented here suggests that the onset of the modern Kyrgyz Tianshan orogeny occurred during the Oligocene–early Miocene (~33–22 Ma) which is coeval with the suggested timing of final closure of the Neo-Tethys at ~35–34 Ma (e.g. Aitchison et al., 2007; Jiang et al., in press) ('hard' India collision in Fig. 6). This timing of basement exhumation has recently been confirmed by several authors for the southern Chinese Tianshan and northern Tarim margin (e.g. ~36 Ma, Yu et al., 2014). More close to the India-Eurasia collision zone, Zhao et al. (2015) recently suggested that the uplift of the Central Lhasa terrane occurred at ~37–30 Ma, indicating that far-field deformation related with the India-Eurasian collision can be traced through the Lhasa terrane, over the northern Tarim margin to the (Kyrgyz) Tianshan. Apparent intensification in basement cooling during the late Miocene (~12–8 Ma) is likely a result of an increased magnitude of shortening (e.g. Sobel et al., 2006; Glorie et al., 2010, 2011a; Macaulay et al., 2014). Given that basement cooling and uplift at that time is abundant throughout most of Central Asia (e.g. uplift of the southern Lhasa terrane at ~15–12 Ma, Zhang et al., 2015; rapid basement cooling at ~13–7 Ma in the northeastern Parmirs, Cao et al., 2013; exhumation in the Zagros belt at ~12–8 Ma, Agard et al., 2011), the intensification of shortening likely affected most of southern Central Asia, possibly as the result of mantle delamination under Tibet and/or the Tianshan (e.g. Li et al., 2009; Molnar and Stock, 2009; Macaulay et al., 2014) and/or the collision of Arabia with Eurasia (e.g. Agard et al., 2011; Chiu et al., 2013; Zhang et al., submitted). This accelerated deformation within Central Asia also coincides with the onset of normal faulting in Tibet (~14 Ma, e.g. Blisniuk et al., 2001) which concurs with the model by Aitken (2011) that the rise and subsequent collapse of Tibet may have contributed to intensified recent deformation into southern Central Asia as well. India-Eurasia convergence is currently ongoing and it has been proposed that subduction of India underneath Eurasia is a chief driving force for this convergence (Capitanio et al., 2010; Müller, 2010). Abdrakhmatov et al. (1996) calculated present-day crustal shortening rates of ~20 mm/yr in the Tianshan, demonstrating that deformation remains very active and even accelerated during the last ~5 Ma, consistent with the Plio–Pleistocene (<5 Ma) intensification of cooling within the Kyrgyz Tianshan.

The lack of late Palaeogene–Neogene thermochronological data for the Siberian Altai-Sayan indicates that the subducting Neo-Tethys and subsequent India-Eurasia collision likely had little to no effect on the modern reactivation of northern Central Asia. Renewed deformation by compressive reactivation of inherited fault systems within the Altai-Sayan is not registered until the Plio–Pleistocene by both thermochronometry as well as structural analysis (e.g. Thomas et al., 2002; Arzhannikova et al., 2011). This Plio–Pleistocene reactivation corresponds with a contemporaneous intensification of rifting in the Baikal region (Petit and Déverchère, 2006; Jolivet et al., 2009). Whereas the India-Eurasia collision itself had likely little influence on the exhumation of the modern Siberian Altai-Sayan, its ongoing convergence, the initiation of the collapse of the Tibetan Plateau and the delamination of lithospheric crust underneath Tibet (discussed above) may have induced the propagation of far-field compressive stresses to the north, reactivating inherited structures within the Siberian Altai-Sayan and within the Baikal region (e.g. Jolivet et al., 2009; Glorie et al., 2012a). Additional tectonic forces such as the rotation and eastward motion of the Amur plate since the Pliocene (e.g. San'kov et al., 2009; Ashurkov et al., 2011; Lee et al., 2011) may however have contributed to the Neogene reactivation of the Altai-Sayan region as well.

The discussed possible links between deformation/exhumation within Central Asia and plate-margin processes are currently only based on coinciding tectonic events that speculate on stress propagation pathways from the plate margins to the Eurasian interior. Our growing understanding of the dynamic history of old (subducted) oceanic plates together with the increasing number of thermochronological data across Central Asia (including Tibet) may potentially allow to model the dynamic response and the stress propagation pathways from the Eurasian margin to the Central Asian continental interior in the future. Given the current existence of significant gaps in the thermochronological data across Central Asia, this modelling approach is not attempted for this paper. Targeting those specific sites for future thermochronological research is therefore the main aim to further test these hypothesised links between the exhumation of Central Asia and the tectonic history of the Eurasian margin, postulated above.

Acknowledgements

This study was supported by grants from the Australian Research Council (DP150101730) and the Fund for Scientific Research, FWO-Vlaanderen. M.M. Buslov, F.I. Zhimulev, V. Yu. Batalev, A. Ryabinin, F. Meeuws, G. Vanbelleghem, W. Vandoorne and B. Jourquin are thanked for their contributions in the field. D. Konopelko and an anonymous reviewer are thanked for their insightful reviews. SG's contribution forms TRaX record #314.

References

Abdrakhmatov, K. Ye, Aldazhanov, S.A., Hager, B.H., Hamburger, M.W., Herring, T.A., Kalabaev, K.B., Makarov, V.I., Molnar, P., Panasyuk, S.V., Prilepin, M.T., Reilinger, R.E., Sadybakasov, I.S., Souter, B.J., Trapeznikov, Tsurkov, Yu, A., Ye, V., Zubovich, A.V., 1996. Relatively recent construction of the Tien Shan inferred from GPS measurements of present-day crustal deformation. Nature 384, 450–453.

Agard, P., Omrani, J., Jolivet, L., Whitechurch, H., Vrielynck, B., Spakman, W., Monié, P., Meyer, B., Wortel, R., 2011. Zagros orogeny: a subduction-dominated process. Geological Magazine 148 (5–6), 692–725.

Aitchison, J.C., Badengzhu, Davis, A.M., Liu, J., Luo, H., Malpas, J.G., McDermid, I.R.C., Wu, H., Ziabrev, S.V., Zhou, M.-F., 2000. Remnants of a cretaceous intra-oceanic subduction system within the Yarlung-Zangbo suture (southern Tibet). Earth and Planetary Science Letters 183, 231–244.

Aitchison, J.C., Ali, J.R., Davis, A.M., 2007. When and where did India and Asia collide? Journal of Geophysical Research 112, B05423.

Aitken, A.R.A., 2011. Did the growth of Tibetan topography control the locus and evolution of Tien Shan mountain building? Geology 39, 459–462.

Alexeiev, D.V., Cook, H.E., Buvtyshkin, V.M., Golub, L.Y., 2009. Structural evoltution of the Ural-Tian Shan junction: a view from Karatau ridge, South Kazakhstan. Comptes Rendus Geoscience 341 (2–3), 287–297.

Allen, M.B., Anderson, L., Searle, R.C., Buslov, M., 2006. Oblique rift geometry of the West Siberian Basin: tectonic setting for the Siberian flood basalts. Journal of the Geological Society of London 163, 901–904.

Arzhannikova, A., Arzhannikov, S., Jolivet, M., Vassallo, R., Chauvet, A., 2011. Pliocene to Quaternary deformation in South East Sayan (Siberia): Initiation of the Tertiary compressive phase in the southern termination of the Baikal Rift System. Journal of Asian Earth Sciences 40 (2), 581–594.

Ashurkov, S.V., San'kov, V.A., Miroschnichenko, A.I., Lukhnev, A.V., Sorokin, A.P., Serov, M.A., Byzov, L.M., 2011. GPS geodetic constraints on the kinematics of the Amurian Plate. Russian Geology and Geophysics 52 (2), 239–249.

Blisniuk, P.M., Hacker, B.R., Glodny, J., Ratschbacher, L., Bi, S., Wu, Z., McWilliams, M.O., Calvert, A., 2001. Normal faulting in central Tibet since at least 13.5 Myr ago. Nature 412, 628–632.
Bouilhol, P., Jagoutz, O., Hanchar, J.M., Dudas, F.O., 2013. Dating the India-Eurasia collision through arc magmatic records. Earth and Planetary Science Letters 366, 163–175.
Bullen, M.E., Burbank, D.W., Garver, J.I., Abdrakhmatov, K,Ye, 2001. Late Cenozoic tectonic evolution of the northwestern Tien Shan: new age estimates for the initiation of mountain building. Geological Society of America Bulletin 113 (12), 1544–1559.
Bullen, M.E., Burbank, D.W., Garver, J.I., 2003. Building the northern Tien Shan: integrated thermal, structural and topographic constraints. Journal of Geology 111, 149–165.
Buslov, M.M., Zykin, V.S., Novikov, I.S., Delvaux, D., 1999. Cenozoic history of the chuya depression (Gorny altai): structure and geodynamics. Russian Geology and Geophysics 40, 1687–1701.
Cao, K., Wang, G.-C., van der Beek, P., Bernet, M., Zhang, K.-X., 2013. Cenozoic thermo-tectonic evolution of the northeastern Pamir revealed by zircon and apatite fission-track thermochronology. Tectonophysics 589, 17–32.
Capitanio, F.A., Morra, G., Goes, S., Weinberg, R.F., Moresi, L., 2010. India–Asia convergence driven by the subduction of the Greater Indian continent. Nature Geoscience 3, 136–139.
Chen, Y., Zhu, D.-C., Zhao, Z.-D., Meng, F.-Y., Wang, Q., Santosh, M., Wang, L.-Q., Dong, G.-C., Mo, X.-X., 2014. Slab breakoff triggered ca. 113Ma magmatism around Xainza area of the Lhasa Terrane, Tibet. Gondwana Research 26 (2), 449–463.
Chiu, H.Y., Chung, S.L., Zarrinkoub, M.H., Mohammadi, S.S., Khatib, M.M., Iizuka, Y., 2013. Zircon U–Pb age constraints from Iran on the magmatic evolution related to Neotethyan subduction and Zagros orogeny. Lithos 162–163, 70–87.
Clark, M.K., 2011. Early Tibetan uplift history eludes. Geology 39, 991–992.
Clark, M.K., Farley, K.A., Zheng, D., Wang, Z., Duvall, A.R., 2010. Early Cenozoic faulting of the northern Tibetan Plateau margin from apatite (U–Th)/He ages. Earth and Planetary Science Letters 296, 78–88.
Clift, P.D., Carter, A., Krol, M., Kirby, E., 2003. Constraints on India-Eurasia collision in the Arabian sea region taken from the Indus group, ladakh Himalaya, India. In: Clift, P.D., Kroon, D., Craig, J., Gaedicke, C. (Eds.), The Tectonic and Climatic Evolution of the Arabian Sea Region, vol. 195. Geological Society of London special publication, pp. 97–116.
Cobbold, P.R., Sadybakasov, E., Thomas, J.C., 1994. Cenozoic Transpression and Basin Development, Kyrghyz Tienshan, Central Asia. In: Roure, F., Ellouz, N., Shein, V.S., Skvortsov, I. (Eds.), Geodynamic Evolution of Sedimentary Basins, International Symposium, pp. 181–202. Moscow.
Cogné, J.P., Kravchinsky, V.A., Halim, N., Hankard, F., 2005. Late Jurassic-Early Cretaceous closure of the Mongol-Okhotsk Ocean demonstrated by new Mesozoic palaeomagnetic results from the Trans-Baikal area (SE Siberia). Geophysical Journal International 163 (2), 813–832.
Davies, C., Allen, M.B., Buslov, M.M., Safonova, I., 2010. Deposition in the kuznetsk Basin, siberia: insights into Permian-Triassic transition and the mesozoic evolution of Central asia. Palaeogeography, Palaeoclimatology, Palaeoecology 295, 307–322.
De Grave, J., Buslov, M.M., Van den haute, P., 2007. Distant effects of India–Eurasia convergence & Mesozoic intracontinental deformation in Central Asia: constraints from apatite fission-track thermochronology. Journal of Asian Earth Sciences 29, 188–204.
De Grave, J., Buslov, M.M., Van den haute, P., Metcalf, J., Dehandschutter, B., Mc Williams, M.O., 2009. Multi-Method chronometry of the Teletskoye graben and its basement, Siberian Altai Mountains: new insights on its thermo-tectonic evolution. In: Lisker, F., Ventura, B., Glasmacher, U.A. (Eds.), Thermochronological methods from palaeotemperature constraints to landscape evolution models, vol. 324. The Geological Society of London Special Publication, pp. 237–259.
De Grave, J., Van den haute, P., 2002. Denudation and cooling of the Lake Teletskoye Region in the Altai Mountains (South Siberia) as revealed by apatite fission-track thermochronology. Tectonophysics 349 (1–4), 145–159.
De Grave, J., Van den Haute, P., Buslov, M.M., Dehandschutter, B., Glorie, S., 2008. Apatite fission-track thermochronology applied to the Chulyshman Plateau, Siberian Altai Region. Radiation Measurements 43 (1), 38–42.
De Grave, J., Glorie, S., Buslov, M.M., Izmer, A., Fournier-Carrie, A., Batalev, V.Y., Vanhaecke, F., Elburg, M.A., Van den Haute, P., 2011. The thermo-tectonic history of the Song-Kul Plateau, Kyrgyz Tien Shan: constraints by apatite and titanite thermochronometry and zircon U/Pb dating. Gondwana Research 20 (4), 745–763.
De Grave, J., Glorie, S., Ryabinin, A., Zhimulev, F., Buslov, M.M., Izmer, A., Elburg, M., Vanhaecke, F., Van den haute, P., 2012. Late palaeozoic and meso-Cenozoic tectonic evolution of the southern kyrgyz Tien Shan: constraints from multi-method thermochronology in the Trans-Alai, Turkestan-Alai section and the Southeastern ferghana Basin. Journal of Asian Earth Sciences 44, 149–168.
De Grave, J., Glorie, S., Buslov, M.M., Stockli, D.F., McWilliams, M.O., Batalev, Yu, V., Van den haute, P., 2013. Thermo-tectonic history of the Issyk-kul basement (Kyrgyz northern Tien Shan, Central asia). Gondwana Research 23, 998–1020.
De Grave, J., De Pelsmaeker, E., Zhimulev, F.I., Glorie, S., Buslov, M.M., Van den haute, P., 2014. Meso-Cenozoic building of the northern Central Asian Orogenic Belt: thermotectonic history of the Tuva region. Tectonophysics 621, 44–59.
De Pelsmaeker, E., Glorie, S., Buslov, M.M., Zhimulev, F.I., Poujol, M., Korobkin, V.V., Vanhaecke, F., Vetrov, E.V., De Grave, J., 2015. Late-Paleozoic emplacement and Meso-Cenozoic reactivation of the southern Kazakhstan granitoid basement. Tectonophysics in press).
Dehandschutter, B., Vysotsky, E., Delvaux, D., Klerkx, J., Buslov, M.M., Seleznev, V.S., De Batist, M., 2002. Structural evolution of the Teletsk graben (Russian Altai). Tectonophysics 351 (1–2), 139–167.
Delvaux, D., Theunissen, K., Van der Meer, R., Berzin, N.A., 1995. Dynamics and paleostress of the Cenozoic Kurai-Chuya depression of Gorny Altai (South Siberia): tectonic and climatic control. Russian Geology and Geophysics 36 (10), 26–45.
Dumitru, T.A., Zhou, D., Chang, E.Z., Graham, S.A., 2001. Uplift, exhumation, and deformation in the Chinese Tian Shan. Geol. Soc. America Memoir 194, 71–99.
Duvall, A.R., Clark, M.K., van der Pluijm, B., Li, C., 2011. Direct dating of Eocene reverse faulting in northeastern Tibet using Ar-dating of fault clays and low-temperature thermochronometry. Earth and Planetary Science Letters 304, 520–526.
Ehlers, T.A., Farley, K.A., 2003. Apatite (U-Th)/He thermochronometry: methods and applications to problems in tectonic and surface processes. Earth and Planetary Science Letters 206 (1–2), 1–14.
England, P., Houseman, G., 1985. Role of lithospheric strength heterogeneities in the tectonics of Tibet and neighbouring regions. Nature 315, 297–301.
Gleadow, A.J.W., Fitzgerald, P.G., 1987. Uplift history and structure of the Transantarctic Mountains: new evidence from fission track dating of basement apatites in the Dry Valley area, southern Victoria Land. Earth and Planetary Science Letters 82, 1–14.
Glorie, S., De Grave, J., Buslov, M.M., Elburg, M.A., Stockli, D.F., Gerdes, A., Van den Haute, P., 2010. Multi-method chronometric constraints on the evolution of the Northern Kyrgyz Tien Shan granitoids (Central Asian Orogenic Belt): from emplacement to exhumation. Journal of Asian Earth Sciences 38 (3–4), 131–146.
Glorie, S., De Grave, J., Buslov, M.M., Zhimulev, F.I., Stockli, D.F., Batalev, V.Y., Izmer, A., Van den haute, P., Vanhaecke, F., Elburg, M., 2011a. Tectonic history of the Kyrgyz South Tien Shan (Atbashi-Inylchek) suture zone: the role of inherited structures during deformation-propagation. Tectonics 30, TC6016.
Glorie, S., De Grave, J., Buslov, M.M., Zhimulev, F.I., Izmer, A., Vandoorne, W., Ryabinin, A., Van den Haute, P., Vanhaecke, F., Elburg, M.A., 2011b. Formation and Palaeozoic evolution of the Gorny-Altai - Altai-Mongolia suture zone (South Siberia): zircon U/Pb constraints on the igneous record. Gondwana Research 20 (2–3), 465–484.
Glorie, S., De Grave, J., Zhimulev, F.I., Buslov, M.M., Elburg, M.A., Van den haute, P., 2012a. Structural control on Meso-Cenozoic tectonic reactivation and denudation in the Siberian Altai: insights from multi-method thermochronometry. Tectonophysics 544–545, 75–92.
Glorie, S., De Grave, J., Delvaux, D., Buslov, M.M., Zhimulev, F.I., Vanhaecke, F., Elburg, M.A., Van den haute, P., 2012b. Tectonic history of the Irtysh shear zone (NE Kazakhstan): new constraints from zircon U/Pb dating, apatite fission track dating and palaeostress analysis. Journal of Asian Earth Sciences 45, 138–149.
Golonka, J., 2004. Plate tectonic evolution of the southern margin of Eurasia in the Mesozoic and Cenozoic. Tectonophysics 381, 235–273.
Golonka, J., Bocharova, N.Y., Ford, D., Edrich, M.E., Bednarczyk, J., Wildharber, J., 2003. Paleogeographic reconstructions and basins development of the Arctic. Marine and Petroleum Geology 20, 211–248.
Harrison, T.M., Copeland, P., Kidd, W.F.S., Yin, A., 1992. Raising tibet. Science 255, 1663–1670.
Hendrix, M.S., Graham, S.A., Carroll, A.R., Sobel, E.R., McKnight, C.L., Shulein, B.J., Wang, Z., 1992. Sedimentary record and climtic implications of recurrent deformation in the Tian Shan: evidence from Mesozoic strata of the north Tarim, south Junggar, and Turpan basins, northwest China. Geological Society of America Bulletin 104, 53–79.
Hetzel, R., Niedermann, S., Tao, M., Kubik, P.W., Ivy-Ochs, S., Gao, B., Strecker, M.R., 2002. Low slip rates and long-term preservation of geomorphic features in Central Asia. Nature 417, 428–432.
Hetzel, R., Dunkl, I., Haider, V., Strobl, M., von Eynatten, H., Ding, L., Frei, D., 2011. Peneplain formation in southern Tibet predates the India-Asia collision and plateau uplift. Geology 39, 983–986.
Jacobs, J., Thomas, R.J., 2001. A titanite fission track profile across the southeastern Archaean Kaapvaal Craton and the Mesoproterozoic Natal Metamorphic Province, South Africa: evidence for differential cryptic meso- to neoproterozoic tectonism. Journal of African Earth Sciences 33 (2), 323–333.
Jiang, T., Aitchison, J.C., Wan, X., 2015. The youngest marine deposits preserved in southern Tibet and disappearance of the Tethyan Ocean. Gondwana Research. http://dx.doi.org/10.1016/j.gr.2015.01.015.
Jolivet, M., Brunel, M., Seward, D., Xu, Z., Yang, J., Roger, F., Tapponnier, P., Malavieille, J., Arnaud, N., Wu, C., 2001. Mesozoic and Cenozoic tectonics of the northern edge of the Tibetan plateau: fission-track constraints. Tectonophysics 343 (1–2), 111–134.
Jolivet, M., Ritz, J.F., Vassallo, R., Larroque, C., Braucher, R., Todbileg, M., Chauvet, A., Sue, C., Arnaud, N., De Vicente, R., Arzhanikova, A., Arzhanikov, S., 2007. Mongolian summits: an uplifted, flat, old but still preserved erosion surface. Geology 35 (10), 871–874.
Jolivet, M., De Boisgrollier, T., Petit, C., Fournier, M., Sankov, V.A., Ringenbach, J.-C., Byzov, L., Miroshnichenko, A.I., Kovalenko, S.N., Anisimova, S.V., 2009. How old is the Baikal Rift Zone? Insight from apatite fission track thermochronology. Tectonics 28, 21.
Jolivet, M., Dominguez, S., Charreau, J., Chen, Y., Li, Y., Wang, Q., 2010. Mesozoic and Cenozoic tectonic history of the central Chinese Tian Shan: reactivated tectonic structures and active deformation. Tectonics 29, 30. TC6019.

Jolivet, M., Heilbronn, G., Robin, C., Barrier, L., Bourquin, S., Guo, Z., Jia, Y., Guerit, L., Yang, W., Fu, B., 2013. Reconstructing the Late Palaeozoic – Mesozoic topographic evolution of the Chinese Tian Shan: available data and remaining uncertainties. Advances in Geosciences 37, 7–18.
Kapp, P., DeCelles, P.G., Gehrels, G.E., Heizler, M., Ding, L., 2007. Geological records of the Lhasa-Qiangtang and Indo-Asian collisions in the Nima area of central Tibet. Geological Society of America Bulletin 119, 917–932.
Ketcham, R.A., 2005. Forward and inverse modelling of low-temperature thermochronometry data. Reviews in Mineralogy and Geochemistry 58, 275–314.
Knapp, J.H., 1996. How earth created heaven. Nature 384, 406–409.
Kohn, B.P., Wagner, M.E., Lutz, T.M., Organist, G., 1993. Anomalous mesozoic Thermal Regime, Central Appalachian-Piedmont – evidence from Sphene and zircon fission-track dating. Journal of Geology 101 (6), 779–794.
Le Heron, D.P., Buslov, M.M., Davies, C., Richards, K., Safonova, I., 2008. Evolution of Mesozoic fluvial systems along the SE flank of the West Siberian Basin, Russia. Sedimentary Geology 208, 45–60.
Lee, G.H., Yoon, Y., Nam, B.H., Lim, H., Kim, Y.-S., Kim, H.J., Lee, K., 2011. Structural evolution of the southwestern margin of the Ulleung Basin, East Sea (Japan Sea) and tectonic implications. Tectonophysics 502 (3–4), 293–307.
Li, Z., Roecker, S., Li, Z., Wei, B., Wang, H., Schelochkov, G., Bragin, V., 2009. Tomographic image of the crust and upper mantle beneath the western Tien Shan from the MANAS broadband deployment: possible evidence for lithospheric delamination. Tectonophysics 477 (1), 49–57.
Lunina, O.V., Gladkov, A.S., Novikov, I.S., Agatova, A.R., Vysotskii, E.M., Emanov, A.A., 2008. Geometry of the fault zone of the 2003 Ms=7.5 Chuya earthquake and associated stress fields, Gorny Altai. Tectonophysics 453 (1–4), 276–294.
Macaulay, E.A., Sobel, E.R., Mikolaichuk, A., Landgraf, A., Kohn, B., Stuart, F., 2013. Thermochronologic insight into late Cenozoic deformation in the basement-cored Terskey Range Kyrgyz Tien Shan. Tectonics 32, 487–500.
Macaulay, E.A., Sobel, E.R., Mikolaichuk, A., Kohn, B., Stuart, F.M., 2014. Cenozoic deformation and exhumation history of the Central Kyrgyz Tien Shan. Tectonics 33, 135–165.
Mahéo, G., Fayoux, X., Guillot, S., Garzanti, E., Capiez, P., Mascle, G., 2006. Relicts of an intra-oceanic arc in the Sapi-Shergol mélange zone (Ladakh, NW Himalaya, India): implications for the closure of the Neo-Tethys Ocean. Journal of Asian Earth Sciences 26 (6), 695–707.
Meneghini, F., Botti, F., Aldega, L., Boschi, C., Carrado, S., Marroni, M., Pandolfi, L., 2012. Hot fluid pumping along shallow-level collisional thrusts: the Monte Rentella shear zone, Umbria Apennine, Italy. Journal of Structural Geology 37, 36–52.
Molnar, P., Stock, J.M., 2009. Slowing of India's convergence with Eurasia since 20 Ma and its implications for Tibetan mantle dynamics. Tectonics 28, TC3001.
Molnar, P., Tapponnier, P., 1975. Cenozoic tectonics of asia: effects of a Continental collision. Science 189, 419–426.
Moore, M.A., England, P.C., 2001. On the inference of denudation rates from cooling ages of minerals. Earth and Planetary Science Letters 185, 265–284.
Müller, D.R., 2010. Sinking continents. Nature Geoscience 3, 79–80.
Najman, Y., Appel, E., Boudagher-Fadel, M., Bown, P., Carter, A., Garzanti, E., Godin, L., Han, J., Liebke, U., Oliver, G., Parrish, R., Vezzoli, G., 2010. Timing of India-Asia collision: geological, biostratigraphic, and palaeomagnetic constraints. Journal of Geophysical Research 115, B12416.
Novikov, I.S., Sokol, E.V., Travin, A.V., Novikova, S.A., 2008. Signature of Cenozoic orogenic movements in combustion metamorphic rocks: mineralogy and geochronology (example of the Salair-Kuznetsk Basin transition). Russian Geology and Geophysics 49, 378–396.
Oskin, M.E., 2012. Tectonics: reanimating eastern tibet. Nature Geoscience 5, 597–598.
Patriat, P., Achache, J., 1984. India–Eurasia collision chronology has implications for crustal shortening and driving mechanism of plates. Nature 311, 615–621.
Petit, C., Déverchère, J., 2006. Structure and evolution of the Baikal rift: a synthesis. Geochemistry, Geophysics,. Geosystems 7, Q11016.
Ratschbacher, L., Hacker, B.R., Webb, L.E., Grimmer, J.C., McWilliams, M.O., Ireland, T., Dong, S., Hu, J.-M., 2003. Tectonics of the Qinling (Central China): tectonostratigraphy, geochronology, and deformation history. Tectonophysics 366, 1–53.
Reiners, P.W., Spell, T.L., Nicolescu, S., Zanetti, K.A., 2004. Zircon (U-Th)/He thermochronometry: He diffusion and comparisons with $^{40}Ar/^{39}Ar$ dating. Geochimica et Cosmochimica Acta 68 (8), 1857–1887.
Roger, F., Jolivet, M., Malavieille, J., 2010. The tectonic evolution of the Songpan-Garzé (North Tibet) and adjacent areas from Proterozoic to Present: a synthesis. Journal of Asian Earth Sciences 39 (4), 254–269.
Rowley, D.B., 1996. Age of initiation of collision between India and Asia: a review of stratigraphic data. Earth and Planetary Science Letters 145, 1–13.
San'kov, V.A., Lukhnev, A.V., Miroshnichenko, A.I., Ashurkov, S.V., Byzov, L.M., Dembelov, M.G., Calais, E., Deverchère, J., 2009. Extension in the Baikal rift: present-day kinematics of passive rifting. Doklady Earth Sciences 425, 205–209.
Sanders, J.S., Long, G.R., 1994. Oil and Gas Resources of the Fergana Basin (Uzbekistan, Tadzhikistan, and Kyrgyzstan). Scientific Report by the Energy Information Administration Office of Oil and Gas. U.S. Dept. Of Energy, Washington, DC.
Schwab, M., Ratschbacher, L., Siebel, W., McWilliams, M., Minaev, V., Lutkov, V., Chen, F., Stanek, K., Nelson, B., Frisch, F., Wooden, J.L., 2004. Assembly of the Pamirs: age and origin of magmatic belts from the southern Tien Shan to the southern Pamirs and their relation to Tibet. Tectonics 23, 31.
Selander, J., Oskin, M., Ormukov, C., Abdrakhmatov, K., 2012. Inherited strike-slip faults as an origin for basement-cored uplifts: example of the Kungey and Zailiskey ranges, northern Tian Shan. Tectonics 31, TC4026.
Sobel, E.R., Oskin, M., Burbank, D., Mikolaichuk, A., 2006. Exhumation of basement-cored uplifts: example of the Kyrgyz Range quantified with apatite fission track thermochronology. Tectonics 25 (2), 1–17.
Stockli, D.F., 2005. Application of low-temperature thermochronometry to extensional tectonic settings. In: Reiners, P.W., Ehlers, T.A. (Eds.), Low-Temperature Thermochronology: Techniques, Interpretations, and Applications. Reviews in Mineralogy and Geochemistry 58, 622.
Stockli, D.F., Farley, K.A., Dumitru, T.A., 2000. Calibration of the apatite (U-Th)/He thermochronometer on an exhumed fault block, White Mountains, California. Geology 28 (11), 983–986.
Sui, Q.-L., Wang, Q., Zhu, D.-C., Zhao, Z.-D., Chen, Y., Santosh, M., Hu, Z.-C., Yuan, H.-L., Mo, X.-X., 2013. Compositional diversity of ca. 110 Ma magmatism in the northern Lhasa Terrane, Tibet: Implications for the magmatic origin and crustal growth in a continent-continent collision zone. Lithos 168, 144–159.
Summerfield, M.A., Brown, R.W., 1998. Geomorphic Factors in the Interpretation of Fission-track Data. In: Van den haute, P., De Corte, F. (Eds.), Advances in Fission-track Geochronology. Kluwer Academic Publishers, Dordrecht, pp. 269–284.
Thomas, J.C., Lanza, R., Kazansky, A., Zykin, V., Semakov, N., Mitrokhin, D., Delvaux, D., 2002. Paleomagnetic study of Cenozoic sediments from the Zaisan basin (SE Kazakhstan) and the Chuya depression (Siberian Altai): tectonic implications for central Asia. Tectonophysics 351 (1–2), 119–137.
Torizin, J., Jentzsch, G., Malischewsky, P., Kley, J., Abakanov, N., Kurskeev, A., 2009. Rating of seismicity and reconstruction of the fault geometries in northern Tien Shan within the project "Seismic Hazard Assessment for Almaty". Journal of Geodynamics 48, 269–278.
Torsvik, T.H., Andersen, T.B., 2002. The Taimyr fold belt, Arctic Siberia: timing of prefold remagnetisation and regional tectonics. Tectonophysics 352, 335–348.
Tshekhovsky, Y.G., Leonov, M.G., 2007. Sedimentary formations and main development stages of the westen Transbaikal and southeastern Baikal regions in the Late Cretaceous and Cenozoic. Lithology and Mineral Resources 42 (4), 349–362.
Valla, P.G., Herman, F., van der Beek, P.A., Braun, J., 2010. Inversion of thermochronological age-elevation profiles to extract independent estimates of denudation and relief history — I: theory and conceptual model. Earth and Planetary Science Letters 295 (3–4), 511–522.
van der Beek, P., Delvaux, D., Andriessen, P.A.M., Levi, K.G., 1996. Early cretaceous denudation related to convergent tectonics in the Baikal region, SE Siberia. Journal of the Geological Society of London 153, 515–523.
van der Beek, P.A., Valla, P.G., Herman, F., Braun, J., Persano, C., Dobson, K.J., Labrin, E., 2010. Inversion of thermochronological age–elevation profiles to extract independent estimates of denudation and relief history — II: application to the French Western Alps. Earth and Planetary Science Letters 296 (1–2), 9–22.
Van Hinsbergen, D.J.J., Lippert, P.C., Dupont-Nivet, G., McQuarrie, N., Doubrovine, P.V., Spakman, W., Torsvik, T.H., 2012. Greater India Basin hypothesis and a two-stage Cenozoic collision between India and Asia. Proceedings of the National Academy of Sciences of the United States of America 109, 7659–7664.
Vassallo, R., Jolivet, M., Ritz, J.-F., Braucher, R., Larroque, C., Sue, C., Todbileg, M., Javkhlanbold, D., 2007. Uplift age and rates of the Gurvan Bogd system (Gobi-Altay) by apatite fission track analysis. Earth and Planetary Science Letters 259 (3–4), 333–346.
Verdel, C., Wernicke, B.P., Hassanzadeh, J., Guest, B., 2011. A Paleogene extensional arc flare-up in Iran. Tectonics 30, TC3008.
Vermeesch, P., 2009. RadialPlotter: a Java application for fission track, luminescence and other radial plots. Radiation Measurements 44, 409–410.
Vyssotski, A.V., Vyssotski, V.N., Nezhdanov, A.A., 2006. Evolution of the west siberian Basin. Marine and Petroleum Geology 23, 93–126.
Wagner, G.A., Van den haute, P., 1992. Fission Track-dating. Kluwer Academic Publishers, Dordrecht, the Netherlands, p. 285.
Walker, R.T., Nissen, E., Molor, E., Bayasgalan, A., 2007. Reinterpretation of the active faulting in central Mongolia. Geology 35, 759–762.
Wang, Q., Zhang, P.-Z., Freymueller, J.T., Bilham, R., Larson, K.M., Lai, X., You, X., Niu, Z., Wu, J., Li, Y., Liu, J., Yang, Z., Chen, Q., 2001. Present-day crustal deformation in China constrained by global positioning system measurements. Science 294, 574.
Wang, Z.X., Li, T., Zhang, J., Liu, Y.Q., Ma, Z.J., 2008. The uplifting process of the Bogda Mountain during the Cenozoic and its tectonic implication. Science in China Series D: Earth Sciences 51, 579–593.
Webb, L.E., Johnson, C.L., 2006. Tertiary strike-slip faulting in southeastern Mongolia and implications for Asian tectonics. Earth and Planetary Science Letters 241, 323–335.
Wolfe, M.R., Stockli, D.F., 2010. Zircon (U-Th)/He thermochronometry in the KTB drill hole, Germany, and its implications for bulk He diffusion kinetics in zircon. Earth and Planetary Science Letters 295 (1–2), 69–82.
Xiao, W., Windley, B.F., Badarch, G., Sun, S., Li, J., Qin, K., Wang, Z., 2004. Palaeozoic accretionary and convergent tectonics of the southern Altaids: implications for the growth of Central Asia. Journal of the Geological Society 161, 339–342.
Xiao, W.J., Huang, B.C., Han, C.M., Sun, S., Li, J.L., 2010. A review of the western part of the Altaids: a key to understanding the architecture of accretionary orogens. Gondwana Research 18, 253–273.

Xiao, W., Windley, B.F., Allen, M.B., Han, C., 2013. Paleozoic multiple accretionary and collisional tectonics of the Chinese Tianshan orogenic collage. Gondwana Research 23, 1316–1341.

Yin, A., Harrison, T.M., 2000. Geological evolution of the Himalayan-Tibetan orogen. Annual Review in Earth and Planetary Sciences 28, 211–280.

Yin, A., Nie, S., Craig, P., Harrison, T.M., Ryerson, F., Qian, X., Yang, G., 1998. Late Cenozoic tectonic evolution of the southern Chinese Tian Shan. Tectonics 17, 1–27.

Yu, S., Chen, W., Evans, N.J., McInnes, B.I.A., Yin, J., Sun, J., Li, J., Zhang, B., 2014. Cenozoic uplift, exhumation and deformation in the north Kuqa Depression, China as constrained by (U–Th)/He thermochronometry. Tectonophysics 630, 166–182.

Yuan, W.M., Carter, A., Dong, J.Q., Bao, Z.K., An, Y.C., Guo, Z.J., 2006. Mesozoic-tertiary exhumation history of the Altai Mountains, northern Xinjiang, China: new constraints from apatite fission track data. Tectonophysics 412 (3–4), 183–193.

Zhai, Q.-G., Jahn, B.-M., Zhang, R.-Y., Wang, J., Su, L., 2011. Triassic subduction of the Paleo-Tethys in northern Tibet, China: evidence from the geochemical and isotopic characteristics of eclogites and blueschists of the Qiangtang block. Journal of Asian Earth Sciences 42, 1356–1370.

Zhang, C.-L., Li, Z.-X., Li, X.-H., Xu, Y.-G., Zhou, G., Ye, H.-M., 2010. A Permian large igneous province in Tarim and Central Asian orogenic belt, NW China: results of a ca. 275 Ma mantle plume? Geological Society of America Bulletin 122, 2020–2040.

Zhang, Z., Xiao, W., Majidifard, M.R., Zhu, R., Ao, S., Wan, B., Chen, L., Rezaeian, M., Esmaeili, R., 2015. A significant younger age of Arabia-Eurasia collision implied by provenance analyses. Geology.

Zhao, J., Qin, K., Li, G., Cao, M., Evans, N.J., McInnes, B.I.A., Li, J., Xiao, B., Chen, L., 2015. The exhumation history of collision-related mineralizing systems in Tibet: insights from thermal studies of the Sharang and Yaguila deposits, central Lhasa. Ore Geology Reviews 65 (4), 1043–1061.